FULL TITLE: *Phlebotomus papatasi* sand fly salivary protein diversity and immune response potential in Egypt and Jordan populations

SHORT TITLE: *Phlebotomus papatasi* salivary protein diversity in ecotopes of Egypt and Jordan

Catherine M. Flanley[1], Marcelo Ramalho-Ortigao[2], Iliano V. Coutinho-Abreu[3], Rami Mukbel[4], Hanafi A. Hanafi[5], Shabaan S. El-Hossary[5], Emadeldin Y. Fawaz[5], David F. Hoel[6], Alexander W. Bray[1], Gwen Stayback[1], Douglas A. Shoue[1], Shaden Kamhawi[3], Scott Emrich[7], Mary Ann McDowell[1*]

[1] Department of Biological Sciences, Eck Institute for Global Health, University of Notre Dame, Notre Dame, IN, United States of America

[2] Department of Preventive Medicine and Biostatistics, F. Edward Hebert School of Medicine, Uniformed Services University of the Health Sciences, Bethesda, Maryland, United States of America

[3] Laboratory of Malaria and Vector Research, NIAID-NIH, Rockville, Maryland, United States of America

[4] Faculty of Veterinary Medicine, Jordan University of Science and Technology, Irbid, Jordan

[5] Vector Biology Research Program, U.S. Naval Medical Research Unit No. 3, Cairo, Egypt

[6] Lee County Mosquito Control District, 15191 Homestead Road, Lehigh Acres, FL 33971

[7] Min H. Kao Department of Electrical Engineering and Computer Science, University of Tennessee, Knoxville, Tennessee, United States of America

[*] Corresponding author

Email: mcdowell.11@nd.edu

Abstract

Phlebotomus papatasi sand flies inject their hosts with a myriad of pharmacologically active salivary proteins to assist with blood feeding and to modulate host defenses. These salivary proteins have been studied for their role in cutaneous leishmaniasis disease outcome with different salivary proteins attenuating or exacerbating lesion size. Studies have shown that while co-administered sand fly saliva exacerbates *Leishmania major* infections in naïve mice, animals pre-exposed to saliva are protected, with the infection attenuated via a delayed-type hypersensitivity immune reaction. These studies highlight the potential of the salivary components to be used as a vaccine. One protein in particular, *P. papatasi* salivary protein 15 (PpSP15) has been intensively studied because of its ability to protect mice against *Le. major* challenge. The number of antigenic molecules included in vaccines is restricted thus emphasizing the role of population genetics to identify molecules, like PpSP15, that are functionally significant, conserved across populations and do not experience selection. Three distinct ecotope study sites, one in Egypt (Aswan) and two in Jordan (Swaimeh and Malka), were chosen based on their elevation, rainfall, vegetation, differing reservoir species, and the presence or absence of *Le. major*. The objective of this work was to analyze the genetic variability of nine of the most abundantly expressed salivary proteins including PpSP12, PpSP14, PpSP28, PpSP29, PpSP30, PpSP32, PpSP36, PpSP42, and PpSP44 and to predict their ability to elicit an immune response. Two proteins, PpSP12 and PpSP14, demonstrated low genetic variability across the three sand fly populations represented in this study, with multiple predicted MHCII epitope binding sites, identified by alleles present in the human populations from the study sites. The other seven salivary proteins revealed greater allelic variation across the same sand fly populations indicating that their use as vaccine targets may prove to be challenging.

Author Summary

Phlebotomus papatasi sand flies vector *Leishmania major* parasites, one of the causative agents of cutaneous leishmaniasis (CL). Approximately 0.7-1.2 million cases of CL occur each year. CL produces disfiguring skin lesions for which no vaccine currently exists. Hematophagous vector salivary proteins are pharmacologically active molecules that modulate inflammation, vasoconstriction, and blood clotting for females that require a sanguineous meal for oviposition. Salivary proteins from multiple phlebotomine sand fly species have been widely studied and scrutinized to characterize their function in blood feeding facilitation as well as their ability to exacerbate or attenuate *Leishmania* infections and their potential as vaccine candidates. A successful sand fly salivary protein-based vaccine to combat CL largely depends on the genetic variability, expression profiles, and human immune response to the salivary proteins selected from geographically distant sand fly populations. The purpose of this study was to analyze these parameters in nine abundantly expressed *P. papatasi* salivary proteins from three distinct ecotopes in Egypt and Jordan in order to assess their potential as vaccine targets

Introduction

Leishmaniasis is a group of neglected diseases caused by *Leishmania* parasites, vectored by phlebotomine sand flies and endemic in 98 countries [1]. Different *Leishmania* species can be or are uniquely associated with distinct clinical outcomes, ranging from cutaneous lesions to fatal visceral disease. Sand flies on the other hand may be specific or not for the transmission of *Leishmania* spp. *Phlebotomus papatasi* sand flies are specific vectors of *Leishmania major*, one of the causative agents of cutaneous leishmaniasis (CL) [2]. Approximately 0.7-1.2 million cases of CL occur each year [1]. CL produces scarring skin lesions and current treatments can be toxic, expensive, require multiple administrations, and can be difficult to access [2]. Although

significant effort has been expended, there currently is no efficacious vaccine for human populations.

Salivary proteins of hematophagous insects are pharmacologically active molecules that modulate inflammation, vasoconstriction, and blood clotting [3]. In *P. papatasi* infected with *Le. major*, parasites are regurgitated into the host's skin during probing or feeding, along with a cocktail of salivary proteins, where an infection can be established. Salivary proteins from various phlebotomine sand fly species have been characterized with regards to their function in blood feeding and their effectiveness as markers of exposure [4–6]. Sand fly salivary proteins can exacerbate or attenuate *Leishmania* infections [7–9], and have been suggested as potential as vaccine candidates [10,11].

It has been previously determined that exposure to uninfected *P. papatasi* bites confers some level of protection against *Le. major* in murine models, presumably via stimulation of a delayed-type hypersensitivity immune response at the site of inoculation [12]. Over thirty different salivary proteins are inoculated into a host with each *P. papatasi* bite [13]. One particular salivary protein, PpSP15, induces a Th-1 mediated immune response with a hallmark increase in IFN-γ in mice [8], and vaccination of nonhuman primates with the *P. duboscqi* orthologous PdSP15 resulted in a significant decrease in parasite load and lesion size, though full protection was not established [10]. Conversely, in naïve hosts, sand fly saliva exacerbates disease progression by downregulating the host's immune response while polarizing the immune response to favor Th2 cytokine production [8,14–16].

Several questions remain concerning the role of sand fly salivary proteins in the epidemiology of leishmaniasis, particularly those pertaining to cross species protection and genetic variability. Cross-protective effects of saliva from different phlebotomine species is

93 another current area of vaccine development research. A cross-protective effect against *Le. major*
94 was demonstrated in mice pre-exposed to uninfected *P. papatasi* sand fly bites and subsequently
95 challenged with *Le. major* plus either *P. papatasi* or *P. duboscqi* salivary gland homogenate [17].
96 Both pre-exposed groups revealed smaller lesion sizes and a decreased parasitic load compared
97 to the unexposed controls [17]. A similar study was conducted with New World sand fly species
98 where hamsters inoculated with *Lu. longipalpis* salivary gland homogenate or a DNA plasmid
99 coding for the highly expressed *Lu. longipalpis* salivary protein LJM19, were protected against
100 challenge with either *Le. braziliensis* and *Lu. longipalpis* salivary gland homogenate, as well as
101 *Le. braziliensis* and *Lu. intermedia* salivary gland homogenate [18].
102 Immunodominant sand fly salivary proteins have also been exploited in epidemiological
103 studies as markers of exposure and risk for *Leishmania* transmission. Anti-saliva antibodies
104 correlate to intensity of exposure with higher anti-saliva antibody titers indicating greater
105 exposure to sand fly bites and a greater probability of transmission [16,19,20]. A disadvantage of
106 measuring antibodies against whole sand fly saliva is the possibility of cross-reactivity between
107 different sand fly species as they may share a significant number of salivary protein antigens.
108 Ideally, a single species-specific salivary protein could be identified to determine exposure and
109 transmission risk (reviewed in [21]). PpSP32, an immunodominant 32 kDa protein present in *P.*
110 *papatasi* saliva, has been validated as an exposure screening tool in Tunisia and Saudi Arabia
111 with no cross-reactivity detected when tested against *P. perniciosus*, a vector of *Le. infantum*,
112 which is also commonly found in sympatry with *P. papatasi* [4,6,22].
113 Genetic variability among populations of sand flies will influence the success of any
114 salivary protein-based vaccine. Specifically, highly polymorphic salivary proteins and those
115 under positive selection should be cautiously considered for further vaccine development.

PpSP15, sampled from sand fly populations in Egypt, Jordan, Saudi Arabia, Israel, and Sudan demonstrated minimal selection with a high degree of conservation at the amino acid level validating PpSP15 as a potential vaccine candidate [23,24]. Here we analyzed the genetic variability of nine highly expressed *P. papatasi* salivary proteins including PpSP12, PpSP14, PpSP28, PpSP29, PpSP30, PpSP32, PpSP36, PpSP42, and PpSP44 from three representative *P. papatasi* populations from Egypt and Jordan.

As a geographically widespread species, *P. papatasi* is prevalent in the Mediterranean Basin, especially the Middle East and North Africa, with an ability to adapt to a variety of habitats that exhibit different climates, elevations, vegetation, and host species. As a result of adaptation to ecological variation, it is expected that sand flies and their salivary proteins face selective pressures that could influence vector competency and disease outcomes [25]. *P. papatasi* population genetics studies have demonstrated that although pockets of genetic variability exist between populations, evidence suggests that the species as a whole remains relatively homogeneous [26–31].

Even so, it remains vitally important to continually monitor salivary protein genetic variability to ensure the most appropriate salivary proteins are chosen as vaccine targets. A successful sand fly salivary protein-based vaccine to combat CL also depends on expression profiles and human (host) immune response to these salivary proteins, ideally selected from geographically distant sand fly populations. Egypt and Jordan are classified as endemic areas for CL, with certain regions designated as hyperendemic in Jordan, with *Le. major* causing the majority of CL cases but *Le. tropica* incriminated in Jordan as well [32,33]. The purpose of this study was to analyze 9 abundantly expressed *P. papatasi* salivary proteins as potential vaccine targets that are conserved across populations from distinct ecotopes in Egypt and Jordan and

demonstrate the potential to elicit an immune response, similar to PpSP15 [24]. We recommend that PpSP12 and PpSP14 also be considered for further vaccine development as we show that they are conserved across populations while also have potential to elicit an immune response. We caution of the use of a highly variable protein like PpSP28 for further development.

Methods

Sand flies

P. papatasi were collected from one field site in each of the following locations: Aswan, Egypt (GPS coordinates N 24°10', E 32°52'), Malka, Jordan (GPS coordinates 31°48', E 35°35'), and Swaimeh, Jordan (N 32°40', E 35°45'), in 2006 and 2007 (Fig 1). Both CO_2 baited (Aswan) and non-baited (Malka and Swaimeh) CDC-style light traps collected sand flies between the hours of 18:00 and 06:00. Three trappings were attempted each year in 2006 and 2007: early (June), middle (August), and late (September). One collection occurred in Malka in late (September) 2006 while three collections occurred in Swaimeh and Aswan in late (September) 2006, early (June), and middle (August) 2007. Sand flies remained alive until dissection and were euthanized in soapy water. Flies were individually identified by microscopic examination of female spermathecae according to Lane [34], and only non-parous females were used in the analysis presented. Parity was assessed according to Anez [35].

Fig 1. *Phlebotomus papatasi* study collection sites.

Map adopted from Wikimedia Commons by Styx under public domain [36].

P. papatasi from Aswan (PPAW) were collected from a small village near the Nile River that permits artificial irrigation for the cultivation of crops like corn (*Zea mays*), wheat (*Triticum*

aestivum), mangoes (*Mangifera indica*), and date palms (*Phoenix dactylifera*). Dogs, goats, and cattle are kept and raised in the village as well. The village sits at 117 m above sea level. Temperatures typically fall between 24° C and 45° C with minimal rainfall. Sand flies are abundant in this village though *Le. major* is absent [37]. *P. papatasi* collected from Swaimeh (PPJS) inhabit an area endemic for zoonotic *Le. major* due to the presence of *Psammomys obesus*, the reservoir host [38]. This low elevation area (~350m below sea level) experiences a Saharan Mediterranean climate with rainfall less than 50mm that occurs from November to April. Temperatures maximally range from 35-40° C in summer months and minimally range from 8-12° C in the winter. The sandy, rocky, salty soil supports halophytic and tropical flora species such as chenopods [39]. *P. papatasi* collected from Malka (PPJM) inhabit a rocky landscape with a typical Mediterranean climate. Malka is located at an elevation of 670 m. During the collection time in 2006, only *Le. tropica* was present in the region and *Le. major* was absent hypothesized due to the absence of *Ps. obesus* [40].

Sample preparation

Dissected, *P. papatasi* female heads with both salivary glands intact were placed in 1.5 ml centrifuge tubes with 50 µL RNA later (Ambion, Austin, TX, USA) and homogenized with an RNAse-free pestle and hand-held homogenizer. Samples were stored at 4° C for up to 48 hours, shipped on dry ice, and then stored at -80° C until analyzed. Table 1 outlines the number of individuals from each site for each salivary protein.

Table 1. *Phlebotomus papatasi* salivary protein amplicon lengths and number of individual sand flies per collection site.

Salivary Protein	Amplicon length (bp)	All	PPAW	PPJM	PPJS
PpSP12	291	96	26	29	41

PpSP14	246	119	29	44	46
PpSP28	554	111	26	30	55
PpSP29	651	126	46	38	42
PpSP30	183	70	20	28	22
PpSP32	568	130	42	45	43
PpSP36	637	82	25	22	35
PpSP42	614	109	27	45	37
PpSP44	675	121	35	44	42

Amplicon lengths = base pairs. PPAW: Aswan, Egypt; PPJM: Malka, Jordan; PPJS: Swaimeh, Jordan.

RNA extraction and cDNA synthesis

Total RNA was extracted from the heads and salivary glands of individual *P. papatasi* samples using the RNeasy Mini RNA isolation kit (Qiagen, Valencia, CA, USA). cDNAs were synthesized using Invitrogen reagents (Invitrogen, Carlsbad, CA, USA), per manufacturer's specifications and briefly outlined in Coutinho-Abreu et al 2011 [41] and Ramalho-Ortigão et al 2015 [24].

Sequence analyses

cDNAs produced from the total RNA of individual *P. papatasi* were amplified by PCR. Primers used to amplify each salivary protein can be found in S1 Table. PCR products were purified by twice washing in 150 µL DNAse/RNAse-free water (Invitrogen, Carlsbad, CA, USA) in Multiscreen PCR cleaning plates (Millipore, Burlington, Massachusetts, USA) with vacuum application (10 psi). Purified PCR products were resuspended in 50 µL sterile water. Leading and lagging strands were sequenced and poor-quality sequences were excluded from the analyses. Forward and reverse chromatograms were inspected and consensus sequences were aligned using MEGA [42] and manually corrected. The resulting sequences were deposited in GenBank (http://ncbi.nlm.nih.gov) and accession numbers can be found in S1 Table.

Multi-copy assessment of salivary proteins

We looked for copy number variation relative to currently assembled *P. papatasi* loci by following the approach of Miles *et al*. [43]. In short, paired sequences from the two individual entries with the most reads (SRR1997534 and SRR199776) were downloaded from SRA. After initial overall quality checking using FastQC [44], these paired reads were then aligned to the Ppap reference assembly using BWA 0.5.9r16 [45]. Next, based on the resulting alignments (SAM output), reads were placed into non-overlapping 300 bp bins such that each bin contained all reads whose alignment started in its corresponding 300 bp interval. Unlike Miles *et al*. [43] there were no known "core genome" coordinates that excluded repeat regions for computing a less biased average count for normalization. Therefore, discrete counts in each bin were normalized based on the average count across all scaffolds, median count, and average count excluding terminal 2 kb of scaffolds (1 kb on 5' and 3' of scaffolds). Although normalization slightly differed, the results in terms of under (less than 0.5 average/median) and over (more than 2 average/median) remained the same within and between the two samples considered. Because of under assembly of heterologous regions, the final normalization value was computed based on the empirical distribution of read bin counts with the value with the greatest number of entries near the computed overall average. Significance was derived using a Poisson model parameterized with this estimate as lambda using the Lander-Waterman model of sequence sampling [46], and a Bonferroni correction was applied to correct for multiple comparisons.

Population analyses

Both interpopulation and intrapopulation analyses were performed using DnaSP v.6 [47]. Interpopulation parameters assessed included: fixation indexes such as Fst [48,49] and Gst [50], as well as Hs and Ks indexes [51]. Other parameters assessed included: neutral evolution hypothesis [52] and neutrality tests Tajima's D [53] and Fu and Li's D and F [54]. The Ka/Ks

ratio (ω) for the whole salivary protein as well as a sliding window analysis of 70 codons each was calculated.

Weblogos [55] pictorially depict the relative frequencies of polymorphic nucleotides and amino acids. The height of the bases indicate relative frequency and conservation is depicted by the overall weight of the stack. Network 5 [56] generated median joining networks exhibiting haplotype relationships.

Secondary structure and T-cell epitope predictions

Secondary structure predictions for each salivary protein were generated using a secondary structure prediction tool (http://bioinf.cs.ucl.ac.uk/psipred) with default parameters based on the consensus sequence for all individual amino acid sequences from DnaSP. Two different predictions tools predicted the promiscuous HLA-class II binding sites and human T-cell epitopes: IEDB analysis resource T-cell epitope prediction tools (http://tools.immuneepitope.org/main/html/tcell_tools.html) [57,58] and ProPred MHC class II binding prediction server (http://www.imtech.res.in/raghava/propred/) [59]. For the 51 HLA alleles tested in ProPred, thresholds included a promiscuous search set to 3%. For the 27 HLA alleles tested in IEDB, only predicted peptides with a Consensus percentile rank of 0.10 or below are included as the top 10% of peptides with the strongest predicted binding affinity.

Results

Using previously published PpSP15 [24] data as a guide to help highlight the proteins presented in this study, we would prioritize PpSP12 and PpSP14 for vaccine development according to our in-depth analyses presented below. The remaining seven salivary proteins may be valid vaccine components; however, the extent of the allelic variation present suggests that their development as vaccine components may prove challenging. Herein, we present data for

PpSP28 as a representative salivary protein with PpSP29, PpSP30, PpSP32, PpSP36, PpSP42, and PpSP44 provided in the supplemental materials.

PpSP12 in-depth analyses

Nucleotide and amino acid genetic diversity. The 291 bp *PpSP12* fragment produced 14 polymorphic sites (Fig 2A). Two specific nucleotide positions indicate limited heterogeneity between the Jordan populations compared to the Egypt population. Position one shows conservation of adenine in both Jordan populations with variation present in the Egypt population. Conversely, in position 13 the conserved frequency of adenine is greater in the Aswan population in comparison to both Malka and Swaimeh. All of the populations present similar heterogeneity at positions 6-9. Although heterogeneity exists in *PpSP12*, it is the lowest when comparing all 9 salivary proteins. The translated PpSP12 amino acid sequence has 6 variable positions out of 97 total amino acids (Fig 2B). At position 2, arginine and lysine are both found in all populations. Both arginine and lysine are positively-charged and belong to the basic group of amino acids. They are frequently substituted for each other in nature [60]. The frequency of alanine and proline are relatively equal for all populations in position 4. Both of these amino acids are small in size, nonpolar, and hydrophobic. At position 3 and 5, the relative frequencies of lysine and asparagine are the same except the Aswan population at position 5 has a much higher frequency of lysine. Lysine is a positively charged polar amino acid and asparagine is polar but neutrally charged. Both are frequently found in protein active, or binding, sites [60].

Fig 2. PpSP12 nucleotide and amino acid variation.

(A) Weblogo illustrating the relative frequencies of nucleotide polymorphisms in wild caught *P. papatasi* populations from PPAW, PPJM, and PPJS. (B) Weblogo illustrating the relative

273 frequencies of amino acid polymorphisms in wild caught *P. papatasi* populations from PPAW,
274 PPJM, and PPJS.

275 **Population genetics analysis.** A total of 96 mature cDNA sequences were analyzed for *PpSP12*
276 from Aswan (n=26), Malka (n=29), and Swaimeh (n=41). Twenty-nine haplotypes were
277 identified with 14 variant sites. Of the 29 haplotypes, 22 were found in only one of the
278 geographic study sites and 6 of the 7 shared haplotypes were found in 2 populations. One
279 haplotype, H_1, was present in all 3 populations and was the most common haplotype. The
280 Aswan, Egypt, population had 5 unique haplotypes (H_2, H_3, H_5, H_8, H_9) with 3 of those
281 being private haplotypes (H_5, H_8, H_9). The Malka, Jordan, population exhibited 9 unique
282 haplotypes (H_10, H_13, H_14, H_15, H_16, H_18, H_19, H_20, H_21) with 6 of the 9 being
283 private haplotypes (H_10, H_14, H_15, H_18, H_19, H_20). The Swaimeh, Jordan, population
284 demonstrated 8 unique haplotypes (H_22 to H_29) with 3 private haplotypes (H_22, H_24,
285 H_25). A variety of population genetics parameters were assessed (Table 2) indicating genetic
286 homogeneity for *PpSP12* across the three populations. Tajima's D and Ka/Ks analysis indicated
287 that this protein is not undergoing positive selection but rather it is either neutral or possibly
288 experiencing purifying selection (Table 2). Furthermore, population structure is not indicated as
289 Fst uncovered little genetic variability in pairwise comparisons (Table 3). The *PpSP12* median-
290 joining network does not demonstrate any notable clustering separating the different populations
291 from one another (Fig 3). Although there are 29 total haplotypes, the haplotypes are
292 differentiated from one another by only one mutation. The Ka/Ks ratio, a diversifying selection
293 index, was 0.293 or less across the sliding window analysis of the protein for all populations
294 indicating purifying or stabilizing selection of this protein (Table 4).
295

296 **Table 2. PpSP12 population genetics analyses for *P. papatasi* populations**

Population	All Data	PPAW	PPJM	PPJS
Number of Sequences	96	26	29	41
Number of Sites	291	291	291	291
- Monomorphic	277	282	281	279
- Polymorphic	14	9	10	12
Singleton variable sites	2	1	0	1
- Site positions	64, 260	260	-	64
Parsimony informative sites	11	8	10	11
- Site positions	36, 54, 74, 75, 108, 117, 124, 126, 138, 150, 252	36, 54, 74, 108, 114, 117, 124, 252	54, 74, 75, 108, 114, 117, 124, 126, 150, 252	36, 54, 74, 75, 108, 114, 117, 124, 126, 138, 252
Segregating sites (S)	14	9	10	12
Total number of mutations (Eta)	16	10	11	12
Total number of synonymous changes	10	5	7	7
- Site positions	36, 54, 75, 108, 114, 114, 114, 126, 138, 150,	36, 54, 108, 114, 114	54, 75, 108, 114, 114, 126, 150	6, 54, 75, 108, 114, 126, 138
Total number of replacement changes	6	5	4	5
- Site positions	64, 74, 117, 124, 252, 260	74, 117, 124, 252, 260	74, 117, 124, 252	64, 74, 117, 124, 252
Number of haplotypes	29	9	14	14
Haplotype diversity (Hd)	0.723	0.58145	0.81307	0.68473
- Standard deviation of Hd	0.034	0.076	0.034	0.055
Nucleotide diversity (Pi)	0.01063	0.00864	0.01139	0.01089
- Standard deviation of Pi	0.00067	0.00135	0.00105	0.00102
Theta (per site) from Eta	0.00943	0.00760	0.00817	0.00828
Theta (per site) from S (Theta-W)	0.00825	0.00684	0.00742	0.00828
- Standard deviation of theta (no recombination)	0.00279	0.00288	0.00300	0.00310
- Standard deviation of	0.00220	0.00228	0.00235	0.00239

theta (free recombination)				
Theta (per site) from Pi	0.01078	0.00874	0.01157	0.01105
Average number of nucleotide differences (k)	3.094	2.51357	3.31579	3.16893
Theta estimated from Eta	2.743	2.21297	2.376	2.411
Fu and Li's D test statistic	-0.72468	0.15876	0.84321	0.86940
- Statistical significance	NS	NS	NS	NS
Fu and Li's F test statistic	-0.38441	0.27545	1.10728	1.02795
- Statistical significance	NS	NS	NS	NS
Tajima's D	0.33033	0.38568	1.12200	0.85937
- Statistical significance	NS	NS	NS	NS
Synonymous sites Tajima's D(Syn)	-0.19687	0.57799	0.16187	0.43992
- Statistical significance	NS	NS	NS	NS
Nonsynonymous sites Tajima's D(Nonsyn)	0.98069	0.07503	2.14787	1.10242
- Statistical significance	NS	NS	NS	NS
Silent sites Tajima's D(Sil)	-0.19687	0.57799	0.16187	0.43992
- Statistical significance	NS	NS	NS	NS
Tajima's D (Nonsyn/Syn) ratio	-4.98139	0.12982	13.26885	2.50597
ω (Ka/Ks)	---	0.222	0.284	0.242

297 NS=p>0.10; NS[1]=0.10 > p > 0.05; *=p<0.05

298

299 **Table 3. *PpSP12* pairwise comparisons of genetic differentiation estimates.**

POP 1	POP 2	Hs	Ks	Gst	Fst	Dxy	Da
PPAW	PPJM	0.70381	2.93656	0.05362	0.06720	0.01074	0.00072
PPAW	PPJS	0.64501	2.91461	0.01242	0.03412	0.01011	0.00034
PPJM	PPJS	0.73758	3.22977	0.02492	-0.00011	0.01114	0.00000

300

Fig 3. Median-joining network for PpSP12 *P. papatasi* haplotypes.

Circle size and circle color indicates frequency and geographical location of haplotypes, respectively. Haplotype numbers are written next to the corresponding circle H_XX. Red numbers between haplotypes indicate number of mutations between haplotypes.

Table 4. PpSP12 sliding window analysis.

	Ka/Ks		
Sliding Window	PPAW	PPJM	PPJS
1-70	0.000	0.000	0.013
71-140	0.293	0.256	0.213
141-210	0.000	0.000	0.000
211-280	----	----	----
281-291	0.000	0.000	0.000

Ka/Ks were plotted for every 70 codons. Values greater than one suggest the potential for positive selection. ---- indicates a lack of polymorphic data in the window to calculate a Ka/Ks value.

Secondary structure & T-cell epitope predictions. The mature amino acid sequence for PpSP12 predicted that only one polymorphic site (R60) was found in an α-helix whereas the other six polymorphic sites were found in predicted coils (D57, K74, A77, K119, N122) (Fig 4). All 6 polymorphic sites are found in predicted MHC II T-cell epitope binding sites though this should not interfere with the potential for T-cell activation as the polymorphic sites are found in the middle of the predicted binding sites and surrounded by conserved regions. Of the 140 amino acids included in this analysis, 95 amino acids were predicted to be potential epitope recognition sites. The areas of the amino acid sequence with the highest predicted binding affinities occur

between the lysine residue at position 2 (K2) and the proline residue at position 23 (P23) as well as the tyrosine residue at position 110 (Y110) and the asparagine residue at position 138 (N138). Of the 78 total HLA alleles tested using the two software tools, all 51 alleles from ProPred identified potential binding sites though certain alleles, such as DRB1_03, DRB1_11, and DRB1_13, had greater binding affinities than the others. The alleles with the strongest binding affinity potential identified by IEDB software included DQA1_0401/DQB1_0402, DPA1_0103/DPB1_0201, and DRB1_0301. The DQA1/DQB1 and DPA1/DPB1 alleles demonstrated a greater affinity for residues between K2 to A20 and DRB1_0301 demonstrated a greater affinity for Y110 to F126, bookending the mature PpSP12.

Fig 4. PpSp12 secondary structure, polymorphic sites, and MHC class II epitope predictions.

The mature PpSP12 amino acid sequence predicted secondary structure. Yellow highlighted amino acids indicate the predicted MHC class II predicted promiscuous peptides. Individual amino acids underlined in black indicate unique polymorphic sites. Predicted secondary structure based on sequence accession #AGE83083[13].

PpSP14 in-depth analyses

Nucleotide and amino acid genetic diversity. The 246-bp *PpSP14* fragment produced 23 polymorphic sites (Fig 5A). Similar to *PpSP12*, there exists limited heterogeneity between the populations studied. Position 11 demonstrates variation in all 3 populations with equal representation of adenine and guanine. In position 17, the Jordan populations have roughly equal rates of cytosine and guanine but the Egypt population has cytosine in the majority. Guanine dominates at position 21 in both Jordan populations but is equally represented with cytosine in

the Egypt population. The remaining 20 polymorphic sites present similar levels of heterogeneity across all 3 populations. The translated PpSP14 amino acid sequence has 14 variable positions out of 82 total amino acids (Fig 5B). At position 1 and 3, leucine, valine, and isoleucine are all easily substituted for one another since they are hydrophobic and prefer to be buried in the protein core. In position 5, the Aswan, Egypt, population demonstrates limited substitution of the asparagine amino acid with lysine, both polar amino acids. Lysine and arginine are relatively equal for all populations at position 8. Lysine and arginine belong to the same basic amino acid group and are known substitutions for one another [60]. Serine and threonine, position 13, are also easily substituted for one another but more threonine is found in the Egypt population compared to the Jordan populations. At position 10, threonine and alanine substitutions are found in all populations but are more frequent in the Egypt population. Even though threonine is polar and alanine is nonpolar, both are small amino acids and threonine's versatility of being inside or outside of the protein, the substitution can be functionally sound. At position 11, threonine is substituted by isoleucine in both Jordanian populations. Even though isoleucine is hydrophobic and threonine is polar, threonine may be on the inside of this protein making this substitution possible, similar to the substitution at position 10 [60].

Fig 5. PpSP14 nucleotide and amino acid variation.

(A) Weblogo illustrating the relative frequencies of nucleotide polymorphisms in wild caught *P. papatasi* populations from PPAW, PPJM, and PPJS. (B) Weblogo illustrating the relative frequencies of amino acid polymorphisms in wild caught *P. papatasi* populations from PPAW, PPJM, and PPJS.

Population genetics analysis. A total of 119 mature cDNA sequences were analyzed for *PpSP14* from PPAW (n=29), PPJM (n=44), and PPJS (n=46). Thirty-eight haplotypes 23 variant

363 sites. Of the 38 haplotypes, 25 were found in only one of the geographic study sites, 8 were
364 shared between PPAW/PPJM or PPJM/PPJS, but none were shared by PPAW/PPJS. Five
365 haplotypes were present in all three populations (H_1, H_5, H_8, H_10, H_13), with H_5 the
366 most common haplotype. PPAW had 6 unique haplotypes (H_3, H_7, H_9, H_11, H_12, H_14)
367 with 1 of those designated a private haplotype (H_3). PPJM had 8 unique haplotypes (H_16,
368 H_18, H_21, H_22, H_23, H_25, H_26, H_27) with 6 of the 8 being private haplotypes (H_16,
369 H_18, H_22, H_23, H_25, H_26). PPJS had 11 unique haplotypes (H_28, H_29, H_30, H_31,
370 H_32, H_33, H_34, H_35, H_36, H_37, H_38) with 6 of the 11 being private haplotypes (H_31,
371 H_32, H_33, H_36, H_37, H_38). The population genetics assessment indicates genetic
372 homogeneity for *PpSP14* across the 3 populations (Table 5). Although the Tajima's D values
373 were negative across all populations, the values were not significant and do not deviate far from
374 zero indicating no selection. The majority of Ka/Ks values are under 1 or do not deviate far from
375 1 further indicating no selection acting on *PpSP14*. There is the potential for population
376 structuring as Fst demonstrated moderate genetic differentiation between PPAW and PPJM
377 (0.10771) and PPAW and PPJS (0.09091) and little genetic differentiation between PPJM and
378 PPJS (0.02346) (Table 6). The *PpSP14* median joining network does not demonstrate any
379 significant clustering separating the different populations from one another (Fig 6). The PPJS
380 haplotypes might be clustering together as compared to PPAW and PPJM but the 38 haplotypes
381 are differentiated from one another by only one mutation. The only exception being haplotypes
382 H_7 and H_12, both from PPAW are differentiated by 3 mutations from one another. The Ka/Ks
383 ratio in the sliding window from 141-210 indicated potential positive selection in both PPJM and
384 PPJS populations but not in the PPAW population (Table 7).
385

386 **Table 5. PpSP14 population genetics analyses for *P. papatasi* populations.**

Population	All Data	PPAW	PPJM	PPJS
Number of Sequences	119	29	44	46
Number of Sites	246	246	246	246
- Monomorphic	223	233	233	232
- Polymorphic	23	13	13	14
Singleton variable sites	2	0	2	1
- Site positions	147, 232	-	147, 232	183
Parsimony informative sites	21	13	11	13
- Site positions	1, 14, 49, 54, 69, 75, 99, 116, 129, 133, 143, 151, 154, 156, 162, 179, 181, 183, 216, 221, 231	1, 14, 49, 99, 129, 143, 154, 156, 162, 179, 181, 183, 221	1, 14, 49, 54, 116, 143, 154, 179, 183, 221, 231	1, 49, 54, 69, 75, 116, 133, 143, 151, 154, 179, 216, 221
Segregating sites (S)	23	13	13	14
Total number of mutations (Eta)	24	14	13	14
Total number of synonymous changes	8	3	4	4
- Site positions	54, 69, 129, 147, 156, 162, 216, 231	129, 156, 162	54, 147, 183, 231	54, 69, 183, 216
Total number of replacement changes	13	8	9	10
- Site positions	1, 14, 49, 75, 99, 116, 133, 143, 151, 154, 179, 221, 232	1, 14, 49, 99, 143, 154, 179, 221	1, 14, 49, 116, 143, 154, 179, 221, 232	1, 49, 75, 116, 133, 143, 151, 154, 179, 221
Number of haplotypes	38	15	20	21
Haplotype diversity (Hd)	0.870	0.876	0.833	0.874
- Standard deviation of Hd	0.013	0.029	0.026	0.019
Nucleotide diversity (Pi)	0.00817	0.00905	0.00657	0.00814
- Standard deviation of Pi	0.00046	0.00102	0.00056	0.00070
Theta (per site) from S (Theta-W)	0.01546	0.01142	0.01047	0.01117
- Standard deviation of	0.00450	0.00430	0.00381	0.00397

theta (no recombination)				
- Standard deviation of theta (free recombination)	0.00322	0.00317	0.00290	0.00299
Theta (per site) from Pi	0.00825	0.00916	0.00663	0.00823
Average number of nucleotide differences (k)	2.009	2.226	1.616	2.003
Theta estimated from Eta	3.969	3.024	2.575	2.749
Fu and Li's D test statistic	0.46088	1.04412	0.35095	0.99210
- Statistical significance	NS	NS	NS	NS
Fu and Li's F test statistic	-0.32793	0.49487	-0.16267	0.43593
- Statistical significance	NS	NS	NS	NS
Tajima's D	-1.33534	-0.78153	-1.02243	-0.75052
- Statistical significance	NS	NS	NS	NS
Synonymous sites Tajima's D(Syn)	-1.63036	-0.83456	-1.08859	-1.12766
- Statistical significance	NS[1]	NS	NS	NS
Nonsynonymous sites Tajima's D(Nonsyn)	-0.63507	-0.12244	-0.76166	-0.40308
- Statistical significance	NS	NS	NS	NS
Silent sites Tajima's D(Sil)	-1.6306	-0.83456	-1.08859	-1.12766
- Statistical significance	NS[1]	NS	NS	NS
Tajima's D (Nonsyn/Syn) ration	0.38953	0.14672	0.69967	0.35745
ω (Ka/Ks)	---	0.877	0.879	1.242

NS=p>0.10; NS[1]=0.10 > p > 0.05; *=p<0.05

Table 6. *PpSP14* pairwise comparisons of genetic differentiation estimates.

POP 1	POP 2	Hs	Ks	Gst	Fst	Dxy	Da
PPAW	PPJM	0.84968	1.85842	0.01880	0.10771	0.00875	0.00094
PPAW	PPJS	0.87453	2.08910	001161	0.09091	0.00945	0.00086
PPJM	PPJS	0.85355	1.81360	0.00205	0.02346	0.00753	0.00018

Fig 6. Median-joining network for PpSP14 *P. papatasi* haplotypes.

Circle size and circle color indicates frequency and geographical location of haplotypes, respectively. Haplotype numbers are written next to the corresponding circle H_XX. Red numbers between haplotypes indicate number of mutations between haplotypes.

Table 7. PpSP14 sliding window analysis.

	Ka/Ks		
Sliding Window	PPAW	PPJM	PPJS
1-70	----	0.322	0.242
71-140	0.748	----	----
141-210	0.541	1.868	14.944
211-246	----	0.330	0.220

Ka/Ks were plotted for every 70 codons. Values greater than one suggest the potential for positive selection. ---- indicates a lack of polymorphic data in the window to calculate a Ka/Ks value.

Secondary structure & T-cell epitope predictions. The mature amino acid sequence for PpSP14 predicted that 6 polymorphic sites (L65, K79, A85, K88, V91, T92) were found in α-helices whereas the other 8 polymorphic sites were found in predicted coils (L41, F45, I57, N73, T100, P101, S114, L118) (Fig 7). Twelve of the 14 polymorphic sites were found in predicted MHC II T-cell epitope binding sites. This variability may affect the predicted binding sites found

between amino acids L41 and K58 and between amino acids L87 and C103, as the variable sites are found at the beginning and end of the fragment. There are no polymorphic sites found between amino acids M1 and F19. The variable sites found between H61 and A77 and I106 and T134 are found in the middle of the amino acid fragment and should not hinder binding. Of the 142 amino acids included in this analysis, 100 amino acids were predicted to be potential epitope recognition sites. The software prediction tools, IEDB and ProPred, agree that the areas of the amino acid sequence with the highest predicted binding affinities occur between methionine residue at position 1 (M1) and the phenylalanine residue at position 19 (F19) as well as the isoleucine residue at position 106 (I106) and the threonine residue at position 134 (T134). Similar to PpSP12, all 51 alleles from ProPred identified potential binding sites, particularly between residues M1 and F19. Alleles DRB1_04XX, DRB1_08XX, DRB1_11XX, DRB1_13XX, and DRB1_15XX had the highest binding affinities overall. To a lesser extent, the following alleles were also identified DRB1_010X, DRB1_030X, DRB1_070X, and DRB5_010X. The alleles with the strongest binding affinity potential identified by IEDB software included DRB3_0101, DPA1_0301/DPB1_0402, DRB1_1101, DAQ1_0101/DQB1_0501, DPA1_0103/DPB1_0201, DRB1_0301, DPA1_0201/DPB1_0101, and DRB5_0101.

Fig 7. PpSp14 secondary structure, polymorphic sites, and MHC class II epitope predictions.

The mature PpSP14 amino acid sequence predicted secondary structure. Yellow highlighted amino acids indicate the predicted MHC class II predicted promiscuous peptides. Individual amino acids underlined in black indicate unique polymorphic sites. Predicted secondary structure based on sequence accession #AGE83089[13].

PpSP28 In-depth Analyses

Nucleotide and amino acid genetic diversity. The 651-bp *PpSP28* fragment produced 95 polymorphic sites (Fig 8A). Approximately, 61% of the polymorphic sites are transition substitutions and 26% are transversions. The remaining 12% of polymorphic sites are mostly conserved as the number of substitutions are so few. Positions 50 and 90 have three possible options at this site, each site a different combination of guanine, cytosine, adenine, or thymine. The translated PpSP28 amino acid sequence has 53 variable positions out of 184 total amino acids (Fig 8B). Eighteen of the variable sites demonstrate limited heterogeneity while the other 35 sites demonstrate significant variation between the populations and an abundance of amino acid substitutions. PpSP28 exhibits the greatest nucleotide and amino acid sequence variability of all 9 salivary proteins studied (Fig 8).

Fig 8. PpSP28 nucleotide and amino acid variation.

(A) Weblogo illustrating the relative frequencies of nucleotide polymorphisms in wild caught *P. papatasi* populations from PPAW, PPJM, and PPJS. (B) Weblogo illustrating the relative frequencies of amino acid polymorphisms in wild caught *P. papatasi* populations from PPAW, PPJM, and PPJS.

Population genetics analysis. A total of 111 mature cDNA sequences were analyzed for *PpSP28* from Aswan (n=26), Malka (n=30), and Swaimeh (n=55). Ninety-five variant sites were identified in 122 haplotypes. Swaimeh, Jordan, tallied the most unique haplotypes (62) with 46 identified as private. Malka, Jordan, had 21 unique haplotypes with 16 identified as private. Aswan, Egypt, totaled 30 unique haplotypes with 24 identified as private. One haplotype was shared by all 3 populations (H_1) and 9 haplotypes were shared by 2 populations. As with *PpSP12* and *PpSP14*, various population genetics parameters were assessed (Table 8) indicating

452 heterogeneity among the populations. Although significant variation is present in *PpSP28*, the
453 analyses do not indicate that positive selection is acting on this salivary protein (Table 8).
454 Population pairwise comparisons, like Fst, reveal great genetic differentiation, according to
455 Wright (1978) between Aswan, Egypt, and Malka, Jordan at 0.10913, and moderate genetic
456 differentiation between Aswan, Egypt, and Swaimeh, Jordan at 0.06936 (Table 9). There is little
457 genetic differentiation between Malka, Jordan, and Swaimeh, Jordan, at 0.01595. The median
458 joining network for *PpSP28* similarly does not exhibit any clear clustering of the Egypt or Jordan
459 populations, but there are as many as 11 mutations separating connected haplotypes (Fig 9).
460 *PpSP28* sliding window analysis of Ka/Ks demonstrates the potential for *PpSP28* to be under
461 diversifying selection in several areas in contrast to the majority of the protein under purifying
462 selection in all populations (Table 10). Values higher than one were detected in all 3 populations
463 with PPJM having two sliding window regions with values over one compared to one sliding
464 window region in PPJS and PPAW (Table 10).

465 **Table 8**. **PpSP28 population genetics analyses for *P. papatasi* populations.**

Population	All Data	PPAW	PPJM	PPJS
Number of Sequences	111	26	30	55
Number of Sites	554	554	554	554
- Monomorphic	495	482	485	475
- Polymorphic	95	72	69	79
Singleton variable sites	9	8	4	5
- Site positions	41, 42, 59, 94, 167, 219, 311, 392, 405	41, 59, 94, 286, 327, 389, 391, 392	8, 70, 157, 391	42, 167, 219, 311, 405
Parsimony informative sites	86	64	65	74
- Site positions	3, 6, 8, 9, 35, 40, 58, 64, 66, 67, 68, 70, 73, 79, 80, 81, 84, 93, 104, 105, 122, 129, 130, 131, 132, 142,	3, 6, 8, 9, 40, 64, 67, 68, 70, 73, 79, 80, 84, 93, 105, 122, 129, 130, 131, 142, 205, 206, 229, 233, 251,	3, 6, 9, 35, 40, 58, 64, 66, 67, 68, 79, 80, 84, 93, 104, 105, 122, 129, 130, 131, 132, 200, 229, 233, 239,	3, 6, 8, 9, 35, 40, 58, 64, 66, 67, 68, 70, 79, 80, 81, 84, 93, 104, 105, 122, 129, 130, 131, 132, 157, 200,

	157, 200, 205, 206, 229, 233, 239, 250, 251, 270, 273, 286, 302, 314, 325, 327, 329, 332, 345, 349, 350, 353, 362, 365, 377, 386, 389, 391, 395, 401, 414, 416, 418, 423, 438, 444, 449, 450, 451, 459, 467, 469, 473, 476, 477, 481, 484, 486, 487, 502, 503, 510, 518, 525, 529, 530, 539, 544 , 552, 553	270, 273, 302, 314, 325, 329, 332, 345, 349, 350, 353, 362, 365, 386, 395, 401, 414, 416, 418, 423, 449, 450, 451, 467, 473, 476, 481, 484, 486, 502, 503, 510, 518, 525, 529, 530, 539, 552, 553	250, 251, 270, 273, 286, 302, 314, 325, 329, 332, 345, 349, 350, 362, 377, 386, 395, 414, 416, 423, 438, 444, 449, 450, 459, 467, 469, 473, 476, 477, 481, 484, 486, 503, 510, 525, 529, 539, 544, 553	229, 233, 239, 251, 270, 273, 286, 302, 314, 325, 327, 329, 332, 345, 349, 350, 362, 377, 386, 389, 395, 414, 416, 423, 438, 444, 450, 451, 459, 467, 469, 473, 476, 477, 481, 484, 486, 487, 502, 503, 510, 518, 525, 529, 530, 539, 552, 553
Segregating sites (S)	95	72	69	79
Total number of mutations (Eta)	107	75	70	88
Total number of synonymous changes	34	27	21	26
- Site positions	35, 41, 59, 80, 104, 122, 122, 167, 200, 206, 233, 239, 251, 302, 311, 314, 332, 353, 362, 365, 377, 386, 386, 389, 392, 395, 401, 416, 423, 449, 467, 518, 525, 539	41, 59, 68, 80, 122, 206, 233, 251, 302, 332, 350, 353, 362, 365, 386, 389, 392, 395, 401, 416, 423, 449, 467, 518, 525, 530, 539	35, 80, 104, 122, 200, 233, 239, 251, 302, 329, 332, 350, 362, 377, 386, 395, 416, 423, 449, 467, 525	35, 80, 104, 122, 122, 167, 200, 233, 239, 251, 302, 311, 314, 332, 362, 377, 386, 386, 389, 395, 416, 423, 467, 518, 525, 530
Total number of replacement changes	52	42	43	44
- Site positions	3, 6, 8, 9, 40, 42, 58, 64, 70, 73, 79, 81, 84, 93, 94, 105, 132, 142, 157, 205, 219, 229, 250, 270, 273, 286, 314, 325,	3, 6, 8, 9, 40, 64, 67, 70, 73, 79, 84, 93, 94, 105, 142, 205, 229, 270, 273, 286, 314, 325, 345, 349, 391, 414, 418, 423,	3, 6, 8, 9, 40, 58, 64, 70, 79, 84, 93, 105, 132, 157, 229, 250, 270, 273, 286, 314, 325, 329, 345, 349, 391, 414, 438,	3, 6, 8, 9, 40, 42, 58, 64, 70, 79, 81, 84, 93, 105, 132, 157, 219, 229, 270, 273, 286, 314, 325, 345, 405, 414, 438, 444,

	345, 391, 405, 414, 418, 423, 438, 444, 450, 451, 459, 469, 473, 476, 477, 481, 484, 486, 487, 510, 539, 544, 552, 553	450, 451, 473, 476, 481, 484, 486, 502, 503, 510, 529, 539, 552, 553	444, 450, 459, 469, 473, 476, 477, 481, 484, 486, 503, 510, 529, 539, 544, 553	450, 451, 459, 469, 473, 476, 477, 481, 484, 486, 487, 510, 529, 539, 552, 553
Number of haplotypes	122	33	28	72
Haplotype diversity (Hd)	0.9881	0.974	0.943	0.991
- Standard deviation of Hd	0.0022	0.00009	0.018	0.003
Nucleotide diversity (Pi)	0.03664	0.03798	0.03276	0.03542
- Standard deviation of Pi	0.00078	0.00114	0.00162	0.00114
Theta (per site) from S (Theta-W)	0.02869	0.02876	0.02671	0.02704
- Standard deviation of theta (no recombination)	0.00666	0.00846	0.00770	0.00703
- Standard deviation of theta (free recombination)	0.00294	0.00339	0.00322	0.00304
Theta (per site) from Pi	0.03852	0.04001	0.03426	0.03718
Average number of nucleotide differences (k)	20.299	21.04223	18.15085	19.623
Theta estimated from Eta	17.900	16.597	15.011	16.688
Fu and Li's D test statistic	0.7669	0.97403	1.56388	1.26815
- Statistical significance	NS	NS	*	NS
Fu and Li's F test statistic	0.71729	1.14769	1.48451	1.16499
- Statistical significance	NS	NS	NS[1]	NS
Tajima's D	0.41277	0.93781	0.71744	0.57070

- Statistical significance	NS	NS	NS	NS
Synonymous sites Tajima's D(Syn)	0.42640	0.61409	0.94295	0.62296
- Statistical significance	NS	NS	NS	NS
Nonsynonymous sites Tajima's D(Nonsyn)	0.87413	1.20554	0.73109	0.77763
- Statistical significance	NS	NS	NS	NS
Silent sites Tajima's D(Sil)	0.42640	0.61409	0.94295	0.62296
- Statistical significance	NS	NS	NS	NS
Tajima's D (Nonsyn/Syn) ration	2.05003	1.96314	0.77532	1.24830
ω (Ka/Ks)	---	0.477	0.487	0.497

NS=p>0.10; NS[1]=0.10 > p > 0.05; *=p<0.05

Table 9. *PpSP28* pairwise comparisons of genetic differentiation estimates.

POP 1	POP 2	Hs	Ks	Gst	Fst	Dxy	Da
PPAW	PPJM	0.95748	19.49328	0.02012	0.10931	0.03971	0.00434
PPAW	PPJS	0.98550	20.07880	0.00712	0.06936	0.03944	0.00274
PPJM	PPJS	0.97399	19.10365	0.01061	0.01595	0.03464	0.00055

Fig 9. Median-joining network for PpSP28 *P. papatasi* haplotypes.

Circle size and circle color indicates frequency and geographical location of haplotypes, respectively. Haplotype numbers are written next to the corresponding circle H_XX. Red numbers between haplotypes indicate number of mutations between haplotypes.

Table 10. PpSP28 sliding window analysis.

	Ka/Ks		
Sliding Window	PPAW	PPJM	PPJS
1-71	1.506	1.329	1.437
72-141	0.624	0.427	0.482

142-211	0.413	0.059	0.254
212-281	0.453	0.473	0.571
282-351	0.852	0.570	0.756
352-421	0.031	0.038	0.024
422-491	0.391	0.890	0.862
492-554	0.845	1.333	0.534

Ka/Ks were plotted for every 70 codons. Values greater than one suggest the potential for positive selection.

Secondary structure & T-cell epitope predictions. The mature amino acid sequence for PpSP28 predicted a total of 53 polymorphic sites with 30 found in α-helices whereas the other 23 polymorphic sites were found in predicted coils (Fig 10). Twenty of the polymorphic sites are found in predicted MHC II T-cell epitope binding sites. Only 1 high affinity predicted binding site between residues M1 and S19 showed no variation. IEDB identified two alleles would recognize this region including DPA1_0301/DPB1_0402 and DPA1_01/DPB1_0401. The majority of the ProPred alleles recognized some combination of residues between M1 and Q28. Another conserved region was identified between residues F33 and S41 and was recognized by DRB1_08XX, DRB1_11XX, and DRB1_13XX. The final region demonstrating conservation between residues L46 and L54 was recognized but by very few alleles. Two of the regions with the strongest affinities housed the most variation such as residues L71 to Q89, with 9 variant sites, and F195 to F203, with 4 variant sites. The high degree of variation within potential epitope binding sites and the decreased variety of alleles identified should exclude PpSP28 from further vaccine development.

Fig 10. PpSp28 secondary structure, polymorphic sites, and MHC class II epitope predictions.

The mature PpSP28 amino acid sequence predicted secondary structure. Yellow highlighted amino acids indicate the predicted MHC class II predicted promiscuous peptides. Individual amino acids underlined in black indicate unique polymorphic sites. Predicted secondary structure based on sequence accession #AGE83090 and #AGE83091[13].

Multi-copy gene analysis for all salivary proteins

Consistent with prior vector genome assemblies, variation within and/or between loci seems to have affected the initial assembly of SP proteins in this species. In general, comparing 2 individual sand fly samples relative to the reference assembly implies that some SP proteins may exist as 2 separate loci given its coverage is significantly less than expected ($p < 0.0002$; see Methods) using the Poisson-based coverage model of Lander and Waterman [46]. The only potential evidence of multiple copies occurred at the 3' terminal end of the second and third region (exon) of SP42 (2-3X expectation in both samples); however, other regions of the same gene were found less than expected ($p < 0.0002$) (S2 Table). We conclude that there is no evidence of over assembly of SP proteins in the current Ppap reference assembly.

Discussion

We examined the genetic variability and potential immunogenicity of nine abundantly expressed *P. papatasi* salivary proteins with the overarching goal of identifying prospective targets to incorporate into an anti-leishmanial vaccine. The salivary proteins assessed included: PpSP12, PpSP14, PpSP28, PpSP29, PpSP30, PpSP32, PpSP36, PpSP42, and PpSP44. All sand flies collected from three natural populations were subjected to similar analyses outlined by Ramalho-Ortigão *et al*. (2015), to ascertain those salivary proteins that demonstrate similar characteristics

515 to PpSP15 as it has been extensively studied as a vaccine target [61]. A multitude of considerations
516 must be addressed to characterize a salivary protein as a potential vaccine candidate, including
517 genetic variability and conservation across populations, consistent expression, and
518 immunogenicity like Th1 vs. Th2 response, and human MHC alleles. We recommend that PpSP12
519 and PpSP14 be considered in vaccination strategies as these proteins are conserved across
520 populations, demonstrate minimal variability, do not appear to be under selective pressure, and
521 have the potential to activate the human immune system. PpSP28, PpSP29, PpSP32, PpSP36,
522 PpSP42, or PpSP44 may be viable candidates for further vaccination applications but we would
523 prioritize PpSP12 and PpSP14.

524 PpSP12 and PpSP14, exhibited a high degree of conservation at the nucleotide and amino
525 acid levels (Figs 2 & 5) across all three populations studied. When our sampled sequences were
526 aligned with previously published *P. papatasi* salivary protein gene sequences from Tunisia
527 (*PpSP12* accession number JQ988874 and *PpSP14* accession number JQ988880)[13] and Israel
528 (*PpSP12* accession number AF335485 and *PpSP14* accession number AF335486)[62], *PpSP12*
529 and *PpSP14* demonstrated almost identical sequences with 95% and 91% percent identity shared,
530 respectively (data not shown). This level of conservation across multiple populations beyond those
531 included in this study demonstrates the potential for a vaccine with broad geographic coverage.
532 Furthermore, the population genetics indices do not indicate that PpSP12 is under selective
533 pressure. PpSP14 might be under slight selective pressure as evidenced by Tajima's D and Ka/Ks
534 ratio though these values are not statistically significant (refer to S39 Table for summary
535 information). In addition, a smaller number of nonsynonymous mutations or replacement changes
536 are observed in PpSP12 (6) and PpSP14 (13) than in previous PpSP15 (19) analysis, further

537 suggesting PpSP12 and PpSP14 are not under positive selection pressures [24]. Nor do the median
538 joining networks utilizing these genes indicate any clear population structuring.

539 PpSP12, PpSp14, and PpSP15 belong to the family of small odorant-binding proteins
540 (OBP) but their specific functions are unknown. *Phlebotomus* OBPs are related to the D7 protein
541 family that includes PpSP28 and PpSP30 and may have arose from a duplication event of a D7
542 gene [13]. The high degree of conservancy among the OBPs demonstrated in this study mimics
543 similar conservation of salivary proteins in geographically distant populations of *P. duboscqi* in
544 Kenya and Mali [63]. *P. duboscqi* and *P. papatasi* belong to the same subgenus and are both known
545 vectors of *Le. major*. The use of highly conserved salivary proteins across sand fly species to elicit
546 a cross-protective effect would make the ideal vaccine, and cross protection against *Le. major*
547 using salivary gland homogenate from *P. papatasi* and *P. duboscqi* using a murine model has been
548 demonstrated [17]. Unfortunately, the same cross-protective phenomenon is not observed in
549 phylogenetically distant species like *P. papatasi* and *Lu. longipalpis* [64]. Even though species
550 specificity exists, cross protection may be possible across species that vector the same *Leishmania*
551 parasites, i.e. *Le. major* vectored by *P. papatasi, P. duboscqi,* and *P. bergeroti*. Cross protection
552 might theoretically be possible against sand flies that vector different *Leishmania* species but
553 results in the same clinical disease outcome. For example, cross protection might be possible
554 between *P. papatasi* and *P. sergenti* that vector *Le. major* and *Le. tropica*, respectively. However,
555 this same phenomenon might not be possible with sand flies that vector *Leishmania* parasites that
556 result in different clinical outcomes (i.e. cutaneous and visceral leishmaniasis) [17].

557 Gene expression is another important consideration in vaccine design as it relates to antigen
558 dosage [65]. Salivary protein genes that are constitutively expressed are viable vaccine targets
559 more so than those genes that change due to seasonality or other factors. Over the course of three

560 sand fly trappings (June, August, September), only *PpSP12* was significantly upregulated in
561 September for the PPJS population but no significant change occurred in the other populations
562 [41]. *PpSP14* did not experience a significant change in expression during the sampling season.
563 Sugar content in plants from dry habitats, like Swaimeh, Jordan, varies in comparison to plants
564 found in irrigated areas like Aswan, Egypt, suggesting that sugar source may be a principle factor
565 in the differential expression demonstrated by *PpSP12*. Gene expression of *PpSP12* and *PpSP14*
566 is influenced by diet and senescence [66]. In colony-reared, 3-day old sand flies, a 3.95 and 2.18-
567 fold change was observed in blood-fed and sugar-fed flies respectively, compared to nonfed sand
568 flies for *PpSP12*. For *PpSP14*, there was a 3.05-fold change in blood fed females compared to
569 nonfed female sand flies. There was similar upregulation of both *PpSP12* and *PpSP14* at day 5
570 and day 9 post-emergence. Though diet and senescence may influence salivary gland gene
571 expression, environmental factors play a much larger role in gene expression regulation in wild
572 populations [66]. Both *PpSP12* and *PpSP14* were expressed throughout seasonal trappings and
573 when specifically tested for age or diet. Although these proteins are not considered constitutively
574 expressed like *PpSP32*, they do not experience downregulation providing further evidence of their
575 potential to provide a high enough antigen dose to prime the immune system for protection [65,66].
576 Another key aspect to vaccine development is the potential to elicit an immune response
577 in human hosts. If certain salivary proteins are not predicted to interface with the appropriate
578 human immune cells, then those salivary proteins should be excluded from further study. Both
579 mature PpSP12 and PpSP14 proteins have multiple promiscuous MHC class II epitopes identified
580 for presentation to T-cell receptors with limited variation in the potential epitope regions.
581 Conversely, PpSP28 demonstrates high variability in predicted epitope regions decreasing the
582 bonding likelihood with MHC class II receptors. We also identified the MHC class II alleles

583 expected to recognize the salivary protein epitopes and investigated the predominant alleles of
584 human populations living in Egypt and Jordan. The MHC class II alleles with strong binding
585 affinities for PpSP12 that are also prevalent in Egyptian and Jordanian human populations include:
586 DRB1_0301, DRB1_040X, DRB1_110X, DRB1_1301, and DRB1_150X [67–69]. The MHC
587 class II alleles identified for PpSP14 include: DRB1_1101, DRB1_0301, DRB1_040X,
588 DRB1_11XX, DRB1_13XX, DRB1_15XX, and to a lesser extent DRB1_070X [67–69]. The six
589 remaining salivary proteins are predicted to bind to MHC class II alleles with varying affinity.
590 PpSP36, PpSp42, and PpSP44 demonstrated greater binding affinities to multiple regions for each
591 predicted protein structure but were not predicted to bind with the most prevalent alleles in the
592 human populations from Egypt and Jordan (data not shown). PpSP29, PpSP30, and PpSP32,
593 displayed fewer predicted binding regions with lower affinities for those regions (data not shown).
594 The data from the prediction software tools adds to the mounting evidence in support of using
595 PpSP12 and PpSP14 in vaccination strategies.

596 Of critical importance is whether these salivary proteins are recognized by human plasma.
597 Although PpSP12 and PpSP14 are smaller in size than the other salivary proteins analyzed, they
598 are less variable overall as there is less opportunity for mutations to occur. Even though larger
599 proteins might be more immunogenic, our data, supported by previous studies, indicate that
600 PpSP12 and PpSP14 will be recognized by alleles circulating in study areas [67–70]. Both PpSP12
601 and PpSP14 are recognized by the immune system but antibody specificity differs among the
602 human populations tested [70]. Our assessment of human responses included Egyptian and
603 Jordanian residents (MENA donors) and U.S. military personnel deployed overseas. Eleven highly
604 expressed salivary proteins were tested for their antibody specificity when compared to controls
605 (i.e., MENA individuals not living in sand fly endemic regions or U.S. military that have not

606 traveled to *P. papatasi*-endemic regions). MENA donors displayed specificity to PpSP12, PpSP26,
607 PpSP30, PpSP38, and PpSP44 but not PpSP14, whereas U.S. military displayed specificity to
608 PpSP14 and PpSP38 but not PpSP12 [70]. In an independent study, it was shown that plasma
609 antibody specificity of 200 Tunisian children ages 6 to 12 years old reacted to PpSP12, PpSP15,
610 PpSP21, PpSP28, PpSP30, PpSP36, and PpSP44, but not to PpSP14 [19], emphasizing the impact
611 of prolonged exposure to sand fly bites versus naïve individuals traveling to sand fly endemic areas
612 [19,70]. Interestingly, PpSP12 and PpSP14 were also shown immunoreactive in unexposed control
613 donors and that the circulating antibodies against these specific salivary proteins could be the result
614 of exposure to other hematophagous arthropod species [70].

615 Specific antibody response also factors into the polarization of the immune response to a
616 Th1-mediated or Th2-mediated response. The polarization to Th1 or Th2 responses result in
617 protection against CL or a disease exacerbation effect, respectively [15,62]. In one study, total *P.*
618 *papatasi* salivary gland homogenate elicited IgG4 specificity as the dominant isotype and subclass
619 circulating in human donors and positively correlated with IgE concentrations [70]. IgG4 and IgE
620 are hallmarks of a Th2 and allergic hypersensitivity response [71]. Another study demonstrated
621 that whole salivary gland homogenate upregulates interleukin 4 (IL-4) while inhibiting interleukin
622 12 (IL-12) and IFN-γ skewing to a Th2 response in the murine model [72]. Th1/Th2 polarization
623 is also dependent on no exposure or pre-exposure to sand fly bites (as reviewed in [73]). The
624 antibody response to individual salivary protein antigens was characterized [19]. PpSP12 was
625 recognized predominately by IgG1 and IgG2 and not IgG4 nor IgE indicating its potential to
626 polarize to a protective Th1 response. PpSP14 was not characterized as it did not demonstrate
627 antibody specificity, but in another study produced a humoral response [8,19].

628 Taken together, our results and those of others demonstrate the potential of PpSP12 and
629 PpSp14 as vaccine targets. Further testing needs to be conducted to more specifically determine
630 the Th1/Th2 response of PpSP12 and PpSP14 as well as determine if these proteins would confer
631 protection in individuals living in endemic regions as well as naïve populations who may work or
632 travel to endemic areas. This work, taken together with other studies, indicates that a combinatorial
633 vaccine comprised of specific salivary proteins and a *Leishmania* parasite antigen would confer a
634 more robust immune response resulting in lasting immunity.

635 ## Funding Statement

636 This project was supported by contract # W911NF0410380 from the Department of
637 Defense (DoD) Defense Advanced Research Projects Agency (DARPA) awarded to MAM.
638 CMF was supported by the University of Notre Dame Eck Institute for Global Health Graduate
639 Student Fellowship, Arthur J. Schmitt Leadership Fellowship in Science and Engineering, and
640 William and Linda Stavropoulos Fellowship in Science.

641 ## Competing Interests

642 The authors declare they have no competing interests.

643 ## Acknowledgments

644 We are grateful to the Egyptian Ministry of Health for their aid and in sand fly collections
645 and the Multi National Force and Observers (MFO) military units for transportation in the Sinai
646 Peninsula. Special gratitude goes to Ms. Maria Badra from U.S. Naval Medical Research Unit
647 Number Three (NAMRU- 3), Cairo, Egypt, for her organizational skills and support of the work
648 in Egypt. The study protocol was approved by the U.S. Naval Medical Research Unit Number
649 Three (NAMRU-3) Institutional Review Board IRB No. 193, DoD No, NAMRU3.2006.0011, in
650 compliance with all applicable Federal regulations governing the protection of human subjects.

The content is solely the responsibility of the authors and does not necessarily represent the official views of the National Institute of Allergy and Infectious Diseases or the National Institutes of Health of the U.S. Department of Defense. DFH is a retired military service member; MRO, IVCA, HAH, SSEH, EEDYF and SK are employees of the U.S. Government. This work was prepared as part of our official duties. Title 17 U.S.C. §105 provides that 'Copyright protection under this title is not available for any work of the United States Government'. Title 17 U.S.C. §101 defines a U.S. Government work as a work prepared by a military service member or employee of the U.S. Government as part of that person's official duties. The opinions and assertions expressed herein are those of the author(s) and do not necessarily reflect the official policy or position of the Uniformed Services University or the Department of Defense. This work was prepared by a military or civilian employee of the U.S. Government as part of the individual's official duties and therefore is in the public domain and does not possess copyright protection. The authors thank Mariha Wadsworth, Jonathon Weyerbacher, and Theresa Lai for their help in the sequencing of the sand fly samples.

1. Alvar J, Vélez ID, Bern C, Herrero M, Desjeux P, Cano J, et al. Leishmaniasis worldwide and global estimates of its incidence. PLoS One. 2012;7. doi:10.1371/journal.pone.0035671

2. World Health Organization. Control of the leishmaniases. World Heal Organ Tech Rep Ser. Geneva; 2010;949: 1–186. doi:10.1038/nrmicro1766

3. Ribeiro JM. Role of saliva in blood feeding by arthropods. Ann Rev Entomol. 1987;32: 463–478. doi:10.1146/annurev.en.32.010187.002335

4. Marzouki S, Abdeladhim M, Abdessalem C Ben, Oliveira F, Ferjani B, Gilmore D, et al. Salivary antigen SP32 is the immunodominant target of the antibody response to

Phlebotomus papatasi bites in humans. PLoS Negl Trop Dis. 2012;6. doi:10.1371/journal.pntd.0001911

5. Sima M, Novotny M, Pravda L, Sumova P, Rohousova I, Volf P. The diversity of yellow-related proteins in sand flies (Diptera: Psychodidae). Traub-Csekö YM, editor. PLoS One. 2016;11: e0166191. doi:10.1371/journal.pone.0166191

6. Marzouki S, Kammoun-Rebai W, Bettaieb J, Abdeladhim M, Hadj Kacem S, Abdelkader R, et al. Validation of recombinant salivary protein PpSP32 as a suitable marker of human exposure to *Phlebotomus papatasi*, the vector of *Leishmania major* in Tunisia. PLoS Negl Trop Dis. 2015;9: 1–14. doi:10.1371/journal.pntd.0003991

7. Valenzuela JG, Garfield M, Rowton ED, Pham VM. Identification of the most abundant secreted proteins from the salivary glands of the sand fly *Lutzomyia longipalpis*, vector of *Leishmania chagasi*. J Exp Biol. 2004;207: 3717–3729. doi:10.1242/jeb.01185

8. Oliveira F, Lawyer PG, Kamhawi S, Valenzuela JG. Immunity to distinct sand fly salivary proteins primes the anti-leishmania immune response towards protection or exacerbation of disease. PLoS Negl Trop Dis. 2008;2. doi:10.1371/journal.pntd.0000226

9. Oliveira F, Jochim RC, Valenzuela JG, Kamhawi S. Sand flies, *Leishmania*, and transcriptome-borne solutions. Parasitol Int. Elsevier B.V.; 2009;58: 1–5. doi:10.1016/j.parint.2008.07.004

10. Oliveira F, Rowton E, Aslan H, Gomes R, Castrovinci PA, Alvarenga PH, et al. A sand fly salivary protein vaccine shows efficacy against vector-transmitted cutaneous leishmaniasis in nonhuman primates. Sci Transl Med. 2015;7: 290ra90. doi:10.1126/scitranslmed.aaa3043

11. Tlili A, Marzouki S, Chabaane E, Abdeladhim M, Kammoun-Rebai W, Sakkouhi R, et al.

Phlebotomus papatasi yellow-related and apyrase salivary proteins are candidates for vaccination against human cutaneous leishmaniasis. J Invest Dermatol. Elsevier; 2017;138: 598–606. doi:10.1016/J.JID.2017.09.043

12. Kamhawi S, Belkaid Y, Modi G, Rowton E, Sacks D. Protection against cutaneous leishmaniasis resulting from bites of uninfected sand flies. Science. 2000;290: 1351–1354. doi:10.1126/science.290.5495.1351

13. Abdeladhim M, Jochim RC, Ben Ahmed M, Zhioua E, Chelbi I, Cherni S, et al. Updating the salivary gland transcriptome of *Phlebotomus papatasi* (Tunisian strain): The search for sand fly-secreted immunogenic proteins for humans. PLoS One. 2012;7: e47347. doi:10.1371/journal.pone.0047347

14. Titus R, Ribeiro J. Salivary gland lysates from the sand fly *Lutzomyia longipalpis* enhance *Leishmania* infectivity. Science (80-). 1988;239: 1306–1308. doi:10.1126/science.3344436

15. Belkaid Y, Kamhawi S, Modi G, Valenzuela J, Noben-Trauth N, Rowton E, et al. Development of a natural model of cutaneous leishmaniasis: Powerful effects of vector saliva and saliva preexposure on the long-term outcome of *Leishmania major* infection in the mouse ear dermis. J Exp Med. 1998;188: 1941–1953. doi:10.1084/jem.188.10.1941

16. Rohousova I, Ozensoy S, Ozbel Y, Volf P. Detection of species-specific antibody response of humans and mice bitten by sand flies. Parasitology. 2005;130: 493–499. doi:10.1017/S003118200400681X

17. Lestinova T, Vlkova M, Votypka J, Volf P, Rohousova I. *Phlebotomus papatasi* exposure cross-protects mice against *Leishmania major* co-inoculated with *Phlebotomus duboscqi* salivary gland homogenate. Acta Trop. 2015;144: 9–18.

720 doi:10.1016/j.actatropica.2015.01.005

721 18. Tavares NM, Silva RA, Costa DJ, Pitombo MA, Fukutani KF, Miranda JC, et al.
722 *Lutzomyia longipalpis* saliva or salivary protein LJM19 protects against *Leishmania*
723 *braziliensis* and the saliva of its vector, *Lutzomyia intermedia*. PLoS Negl Trop Dis.
724 2011;5. doi:10.1371/journal.pntd.0001169

725 19. Marzouki S, Ben Ahmed M, Boussoffara T, Abdeladhim M, Ben Aleya-Bouafif N,
726 Namane A, et al. Characterization of the antibody response to the saliva of *Phlebotomus*
727 *papatasi* in people living in endemic areas of cutaneous leishmaniasis. Am J Trop Med
728 Hyg. 2011;84: 653–661. doi:10.4269/ajtmh.2011.10-0598

729 20. de Moura TR, Oliveira F, Novais FO, Miranda JC, Clarêncio J, Follador I, et al. Enhanced
730 *Leishmania braziliensis* infection following pre-exposure to sandfly saliva. PLoS Negl
731 Trop Dis. 2007;1. doi:10.1371/journal.pntd.0000084

732 21. Andrade BB, Teixeira CR. Biomarkers for exposure to sand flies bites as tools to aid
733 control of leishmaniasis. Front Immunol. 2012;3: 1–7. doi:10.3389/fimmu.2012.00121

734 22. Mondragon-Shem K, Al-Salem WS, Kelly-Hope L, Abdeladhim M, Al-Zahrani MH,
735 Valenzuela JG, et al. Severity of Old World cutaneous leishmaniasis is influenced by
736 previous exposure to sandfly bites in Saudi Arabia. PLoS Negl Trop Dis. 2015;9:
737 e0003449. doi:10.1371/journal.pntd.0003449

738 23. Elnaiem D-EA, Meneses C, Slotman M, Lanzaro GC. Genetic variation in the sand fly
739 salivary protein, SP-15, a potential vaccine candidate against *Leishmania major*. Insect
740 Mol Biol. 2005;14: 145–150. doi:10.1111/j.1365-2583.2004.00539.x

741 24. Ramalho-Ortigão M, Coutinho-Abreu I V., Balbino VQ, Figueiredo CAS, Mukbel R,
742 Dayem H, et al. *Phlebotomus papatasi* SP15: mRNA expression variability and amino

743 acid sequence polymorphisms of field populations. Parasit Vectors. 2015;8: 298.
744 doi:10.1186/s13071-015-0914-2
745 25. Coutinho-Abreu I V., Ramalho-Ortigao M. Ecological genomics of sand fly salivary gland
746 genes: An overview. J Vector Ecol. 2011;36: 58–63. doi:10.1111/j.1948-
747 7134.2011.00112.x
748 26. Hamarsheh O, Presber W, Abdeen Z, Sawalha S, Al-Lahem A, Schönian G. Genetic
749 structure of Mediterranean populations of the sandfly *Phlebotomus papatasi* by
750 mitochondrial cytochrome b haplotype analysis. Med Vet Entomol. 2007;21: 270–277.
751 doi:10.1111/j.1365-2915.2007.00695.x
752 27. Hamarsheh O, Presber W, Yaghoobi-Ershadi MR, Amro A, Al-Jawabreh A, Sawalha S, et
753 al. Population structure and geographical subdivision of the *Leishmania major* vector
754 *Phlebotomus papatasi* as revealed by microsatellite variation. Med Vet Entomol. 2009;23:
755 69–77. doi:10.1111/j.1365-2915.2008.00784.x
756 28. Depaquit J, Lienard E, Verzeaux-Griffon A, Ferté H, Bounamous A, Gantier JC, et al.
757 Molecular homogeneity in diverse geographical populations of *Phlebotomus papatasi*
758 (Diptera, Psychodidae) inferred from ND4 mtDNA and ITS2 rDNA. Epidemiological
759 consequences. Infect Genet Evol. 2008;8: 159–170. doi:10.1016/j.meegid.2007.12.001
760 29. Esseghir S, Ready PD, Killick-Kendrick R, Ben-Ismail R. Mitochondrial haplotypes and
761 phylogeography of *Phlebotomus* vectors of *Leishmania major*. Insect Mol Biol. 1997;6:
762 211–225. doi:DOI 10.1046/j.1365-2583.1997.00175.x
763 30. Raja B, Jaouadi K, Haouas N, Mezhoud H, Bdira S, Amor S. Mitochondrial cytochrome b
764 variation in populations of the cutaneous leishmaniasis vector *Phlebotomus papatasi*
765 across eastern Tunisia. Int J Biodivers Conserv. 2012;4: 189–196.

doi:10.5897/IJBC11.191

31. Flanley CM, Ramalho-Ortigao M, Coutinho-Abreu I V, Mukbel R, Hanafi HA, El-Hossary SS, et al. Population genetics analysis of *Phlebotomus papatasi* sand flies from Egypt and Jordan based on mitochondrial cytochrome b haplotypes. Parasit Vectors. 2018;11: 1–11. doi:10.1186/s13071-018-2785-9

32. Bessat M, Shanat S El. Leishmaniasis: Epidemiology, control and future perspectives with special emphasis on Egypt. J Trop Dis. 2015;2: 1–10. doi:10.4172/2329891X.1000153

33. Salam N, Al-Shaqha WM, Azzi A. Leishmaniasis in the Middle East: Incidence and epidemiology. PLoS Negl Trop Dis. 2014;8: 1–8. doi:10.1371/journal.pntd.0003208

34. Lane RP. The sandflies of Egypt (Diptera: Phlebotominae). Bull Br Museum (Natural Hist. London: The Museum; 1986;52: 1–35.

35. Añez N, Tang Y. Comparison of three methods for age-grading of female Neotropical phlebotomine sandflies. Med Vet Entomol. 1997;11: 3–7. doi:10.1111/j.1365-2915.1997.tb00283.x

36. STyx. World Location Map. In: Wikimedia Commons [Internet]. 2010. Available: https://commons.wikimedia.org/wiki/File:World_location_map.svg

37. Hoel DF, Butler JF, Fawaz EY, Watany N, El-Hossary SS, Villinski J. Response of phlebotomine sand flies to light-emitting diode-modified light traps in southern Egypt. J Vector Ecol. 2007;32: 302–8. doi:10.3376/1081-1710(2007)32[302:ROPSFT]2.0.CO;2

38. Saliba EK, Oumeish OY. Reservoir hosts of cutaneous leishmaniasis. Clin Dermatol. 1999;17: 275–277. doi:10.1016/S0738-081X(99)00045-0

39. Schlein Y, Jacobson RL. Linkage between susceptibility of *Phlebotomus papatasi* to *Leishmania major* and hunger tolerance. Parasitology. 2002;125: 343–8.

789 doi:10.1017/S0031182002002147

790 40. Kamhawi S, Modi GB, Pimenta PF, Rowton E, Sacks DL. The vectorial competence of
791 *Phlebotomus sergenti* is specific for *Leishmania tropica* and is controlled by species-
792 specific, lipophosphoglycan-mediated midgut attachment. Parasitology. 2000;121: 25–33.
793 doi:10.1017/S0031182099006125

794 41. Coutinho-Abreu I V, Mukbel R, Hanafi HA, Fawaz EY, El-Hossary SS, Wadsworth M, et
795 al. Expression plasticity of *Phlebotomus papatasi* salivary gland genes in distinct ecotopes
796 through the sand fly season. BMC Ecol. BioMed Central Ltd; 2011;11: 24.
797 doi:10.1186/1472-6785-11-24

798 42. Kumar S, Stecher G, Tamura K. MEGA7: Molecular evolutionary genetics analysis
799 version 7.0 for bigger datasets. Mol Biol Evol. 2016;33: 1870–1874.
800 doi:10.1093/molbev/msw054

801 43. Miles A, Iqbal Z, Vauterin P, Pearson R, Campino S, Theron M, et al. Indels, structural
802 variation, and recombination drive genomic diversity in *Plasmodium falciparum*. Genome
803 Res. 2016;26: 1288–1299. doi:10.1101/gr.203711.115

804 44. Andrews S. FastQC: a quality control tool for high throughput sequence data. [Internet].
805 2010. Available: https://www.bioinformatics.babraham.ac.uk/projects/fastqc/

806 45. Li H, Durbin R. Fast and accurate long-read alignment with Burrows-Wheeler transform.
807 Bioinformatics. 2010;26: 589–595. doi:10.1093/bioinformatics/btp698

808 46. Lander ES, Waterman MS. Genomic mapping by fingerprinting random clones: A
809 mathematical analysis. Genomics. 1988;2: 231–239. doi:10.1016/0888-7543(88)90007-9

810 47. Rozas J, Ferrer-Mata A, Sanchez-DelBarrio JC, Guirao-Rico S, Librado P, Ramos-Onsins
811 SE, et al. DnaSP 6: DNA sequence polymorphism analysis of large data sets. Mol Biol

812 Evol. Oxford University Press; 2017;34: 3299–3302. doi:10.1093/molbev/msx248

813 48. Hudson RR, Slatkin M, Maddison WP. Estimation of levels of gene flow from DNA
814 sequence data. Genetics. 1992;132: 583–589. doi:PMC1205159

815 49. Wright S. Evolution and the genetics of populations, variability within and among natural
816 populations. The University of Chicago Press, Chicago. 1978.

817 50. Nei M. Analysis of gene diversity in subdivided populations. Proc Natl Acad Sci U S A.
818 1973;70: 3321–3323. doi:10.1073/pnas.70.12.3321

819 51. Hudson RR, Boos DD, Kaplan NL. A statistical test for detecting geographic subdivision.
820 Mol Biol Evol. 1992;9: 138–151.

821 52. Kimura M. Evolutionary rate at the molecular level. Nature. 1968;217: 624–626.
822 doi:10.1038/217624a0

823 53. Tajima F. Statistical method for testing the neutral mutation hypothesis by DNA
824 polymorphism. Genetics. 1989;123: 585–595. doi:PMC1203831

825 54. Fu YX, Li WH. Statistical tests of neutrality of mutations. Genetics. 1993;133: 693–709.

826 55. Crooks G, Hon G, Chandonia J, Brenner S. WebLogo: a sequence logo generator.
827 Genome Res. 2004;14: 1188–1190. doi:10.1101/gr.849004.1

828 56. Bandelt HJ, Forster P, Röhl A. Median-joining networks for inferring intraspecific
829 phylogenies. Mol Biol Evol. 1999;16: 37–48. doi:10.1093/oxfordjournals.molbev.a026036

830 57. Wang P, Sidney J, Dow C, Mothé B, Sette A, Peters B. A systematic assessment of MHC
831 class II peptide binding predictions and evaluation of a consensus approach. PLoS
832 Comput Biol. 2008;4. doi:10.1371/journal.pcbi.1000048

833 58. Wang P, Sidney J, Kim Y, Sette A, Lund O, Nielsen M, et al. Peptide binding predictions
834 for HLA DR, DP and DQ molecules. BMC Bioinformatics. 2010;11: 568–580.

doi:10.1186/1471-2105-11-568

59. Singh H, Raghava GPS. ProPred: Prediction of HLA-DR binding sites. Bioinformatics. 2001;17: 1236–1237. doi:10.1093/bioinformatics/17.12.1236

60. Betts MJ, Russell RB. Amino acid properties and consequences of substitutions. In: Barnes MR, Gray IC, editors. Bioinformatics for Geneticists. West Sussex: John Wiley & Sons Ltd.; 2003. pp. 289–304. doi:10.1002/0470867302.ch14

61. Srivastava S, Shankar P, Mishra J, Singh S. Possibilities and challenges for developing a successful vaccine for leishmaniasis. Parasites and Vectors. 2016;9: 1–15. doi:10.1186/s13071-016-1553-y

62. Valenzuela JG, Belkaid Y, Garfield MK, Mendez S, Kamhawi S, Rowton ED, et al. Toward a defined anti-*Leishmania* vaccine targeting vector antigens: Characterization of a protective salivary protein. J Exp Med. 2001;194: 331–342. doi:10.1084/jem.194.3.331

63. Kato H, Anderson JM, Kamhawi S, Oliveira F, Lawyer PG, Pham VM, et al. High degree of conservancy among secreted salivary gland proteins from two geographically distant *Phlebotomus duboscqi* sandflies populations (Mali and Kenya). BMC Genomics. 2006;7: 1–21. doi:10.1186/1471-2164-7-226

64. Thiakaki M, Rohousova I, Volfova V, Volf P, Chang KP, Soteriadou K. Sand fly specificity of saliva-mediated protective immunity in *Leishmania amazonensis*-BALB/c mouse model. Microbes Infect. 2005;7: 760–766. doi:10.1016/j.micinf.2005.01.013

65. Henrickson SE, Mempel TR, Mazo IB, Liu B, Artyomov MN, Zheng H, et al. T cell sensing of antigen dose governs interactive behavior with dendritic cells and sets a threshold for T cell activation. Nat Immunol. 2008;9: 282–291. doi:10.1038/ni1559

66. Coutinho-Abreu I V, Wadsworth M, Stayback G, Ramalho-Ortigao M, McDowell MA.

Differential expression of salivary gland genes in the female sand fly P*hlebotomus papatasi* (Diptera: Psychodidae). J Med Entomol. 2010;47: 1146–1155. doi:10.1603/ME10072

67. Hajjej A, Almawi WY, Arnaiz-Villena A, Hattab L, Hmida S. The genetic heterogeneity of Arab populations as inferred from HLA genes. PLoS One. 2018;13: 1–24. doi:10.1371/journal.pone.0192269

68. González-Galarza FF, Takeshita LYC, Santos EJM, Kempson F, Maia MHT, da Silva ALS, et al. Allele frequency net 2015 update: New features for HLA epitopes, KIR and disease and HLA adverse drug reaction associations. Nucleic Acids Res. 2015;43: D784–D788. doi:10.1093/nar/gku1166

69. Elbjeirami WM, Abdel-Rahman F, Hussein AA. Probability of finding an HLA-matched donor in immediate and extended families: The Jordanian experience. Biol Blood Marrow Transplant. 2013;19: 221–226. doi:10.1016/j.bbmt.2012.09.009

70. Geraci NS, Mukbel RM, Kemp MT, Wadsworth MN, Lesho E, Stayback GM, et al. Profiling of human acquired immunity against the salivary proteins of *Phlebotomus papatasi* reveals clusters of differential immunoreactivity. Am J Trop Med Hyg. 2014;90: 923–938. doi:10.4269/ajtmh.13-0130

71. Punnonen J, Aversa G, Cocks BG, McKenzie AN, Menon S, Zurawski G, et al. Interleukin 13 induces interleukin 4-independent IgG4 and IgE synthesis and CD23 expression by human B cells. Proc Natl Acad Sci. 1993;90: 3730–3734. doi:10.1073/pnas.90.8.3730

72. Mbow ML, Bleyenberg JA, Hall LR, Titus RG. *Phlebotomus papatasi* sand fly salivary gland lysate down-regulates a Th1, but up-regulates a Th2, response in mice infected with

Leishmania major. J Immunol. 1998;161: 5571–7.

73. Lestinova T, Rohousova I, Sima M, de Oliveira CI, Volf P. Insights into the sand fly saliva: Blood-feeding and immune interactions between sand flies, hosts, and *Leishmania*. PLoS Negl Trop Dis. 2017;11: 1–26. doi:10.1371/journal.pntd.0005600

S1 Table. *Phlebotomus papatasi* salivary protein primers and GenBank accession numbers.

***=Amplicon is under 200 base pairs; not assigned an accession number; sequences available upon request.

S2 Table. *Phlebotomus papatasi* salivary protein gene multi-copy assessment.

S3 Fig. PpSP29 nucleotide and amino acid variation.

(A) Weblogo illustrating the relative frequencies of nucleotide polymorphisms in wild caught *P. papatasi* populations from PPAW, PPJM, and PPJS. (B) Weblogo illustrating the relative frequencies of amino acid polymorphisms in wild caught *P. papatasi* populations from PPAW, PPJM, and PPJS.

S4 Table. **PpSP29 population genetics analyses for *P. papatasi* populations**

NS=$p>0.10$; NS[1]=$0.10 > p > 0.05$; *=$p<0.05$

S5 Table. *PpSP29* pairwise comparisons of genetic differentiation estimates.

S6 Fig. Median-joining network for PpSP29 *P. papatasi* haplotypes.

Circle size and circle color indicates frequency and geographical location of haplotypes, respectively. Haplotype numbers are written next to the corresponding circle H_XX. Red numbers between haplotypes indicate number of mutations between haplotypes.

S7 Table. PpSP29 sliding window analysis.

Ka/Ks were plotted for every 70 codons. Values greater than one suggest the potential for positive selection. ---- indicates a lack of polymorphic data in the window to calculate a Ka/Ks value.

S8 Fig. PpSp29 secondary structure, polymorphic sites, and MHC class II epitope predictions.

The mature PpSP29 amino acid sequence predicted secondary structure. Yellow highlighted amino acids indicate the predicted MHC class II predicted promiscuous peptides. Individual amino acids underlined in black indicate unique polymorphic sites. Predicted secondary structure based on sequence accession #AGE83096[13].

S9 Fig. PpSP30 nucleotide and amino acid variation.

(A) Weblogo illustrating the relative frequencies of nucleotide polymorphisms in wild caught *P. papatasi* populations from PPAW, PPJM, and PPJS. (B) Weblogo illustrating the relative frequencies of amino acid polymorphisms in wild caught *P. papatasi* populations from PPAW, PPJM, and PPJS.

927 **S10 Table**. **PpSP30 population genetics analyses for *P. papatasi* populations**

928 NS=p>0.10; NS[1]=0.10 > p > 0.05; *=p<0.05

929

930 **S11 Table. *PpSP30* pairwise comparisons of genetic differentiation estimates.**

931

932 **S12 Fig. Median-joining network for PpSP30 *P. papatasi* haplotypes.**

933 Circle size and circle color indicates frequency and geographical location of haplotypes,

934 respectively. Haplotype numbers are written next to the corresponding circle H_XX. Red

935 numbers between haplotypes indicate number of mutations between haplotypes.

936

937 **S13 Table. PpSP30 sliding window analysis.**

938 Ka/Ks were plotted for every 70 codons. Values greater than one suggest the potential for

939 positive selection. ---- indicates a lack of polymorphic data in the window to calculate a Ka/Ks

940 value.

941

942 **S14 Fig. PpSp30 secondary structure, polymorphic sites, and MHC class II epitope**

943 **predictions.**

944 The mature PpSP30 amino acid sequence predicted secondary structure. Yellow highlighted

945 amino acids indicate the predicted MHC class II predicted promiscuous peptides. Individual

946 amino acids underlined in black indicate unique polymorphic sites. Predicted secondary structure

947 based on sequence accession #AGE83093[13].

948

949 **S15 Fig. PpSP32 nucleotide and amino acid variation.**

(A) Weblogo illustrating the relative frequencies of nucleotide polymorphisms in wild caught *P. papatasi* populations from PPAW, PPJM, and PPJS. (B) Weblogo illustrating the relative frequencies of amino acid polymorphisms in wild caught *P. papatasi* populations from PPAW, PPJM, and PPJS.

S16 Table. **PpSP32 population genetics analyses for *P. papatasi* populations**

NS=$p>0.10$; NS[1]=$0.10 > p > 0.05$; *=$p<0.05$

S17 Table. *PpSP32* pairwise comparisons of genetic differentiation estimates.

S18 Fig. Median-joining network for PpSP32 *P. papatasi* haplotypes.

Circle size and circle color indicates frequency and geographical location of haplotypes, respectively. Haplotype numbers are written next to the corresponding circle H_XX. Red numbers between haplotypes indicate number of mutations between haplotypes.

S19 Table. PpSP32 sliding window analysis.

Ka/Ks were plotted for every 70 codons. Values greater than one suggest the potential for positive selection. ---- indicates a lack of polymorphic data in the window to calculate a Ka/Ks value.

S20 Fig. PpSp32 secondary structure, polymorphic sites, and MHC class II epitope predictions.

The mature PpSP32 amino acid sequence predicted secondary structure. Yellow highlighted amino acids indicate the predicted MHC class II predicted promiscuous peptides. Individual amino acids underlined in black indicate unique polymorphic sites. Predicted secondary structure based on sequence accession #AGE83097[13].

S21 Fig. PpSP36 nucleotide and amino acid variation.

(A) Weblogo illustrating the relative frequencies of nucleotide polymorphisms in wild caught *P. papatasi* populations from PPAW, PPJM, and PPJS. (B) Weblogo illustrating the relative frequencies of amino acid polymorphisms in wild caught *P. papatasi* populations from PPAW, PPJM, and PPJS.

S22 Table. **PpSP36 population genetics analyses for *P. papatasi* populations**

NS=$p>0.10$; NS[1]=$0.10 > p > 0.05$; *=$p<0.05$

S23 Table. *PpSP36* pairwise comparisons of genetic differentiation estimates.

S24 Fig. Median-joining network for PpSP36 *P. papatasi* haplotypes.

Circle size and circle color indicates frequency and geographical location of haplotypes, respectively. Haplotype numbers are written next to the corresponding circle H_XX. Red numbers between haplotypes indicate number of mutations between haplotypes.

S25 Table. PpSP36 sliding window analysis.

994 Ka/Ks were plotted for every 70 codons. Values greater than one suggest the potential for
995 positive selection. ---- indicates a lack of polymorphic data in the window to calculate a Ka/Ks
996 value.
997
998 **S26 Fig. PpSp36 secondary structure, polymorphic sites, and MHC class II epitope**
999 **predictions.**
1000 The mature PpSP36 amino acid sequence predicted secondary structure. Yellow highlighted
1001 amino acids indicate the predicted MHC class II predicted promiscuous peptides. Individual
1002 amino acids underlined in black indicate unique polymorphic sites. Predicted secondary structure
1003 based on sequence accession #AGE83101[13].
1004
1005 **S27 Fig. PpSP42 nucleotide and amino acid variation.**
1006 (A) Weblogo illustrating the relative frequencies of nucleotide polymorphisms in wild caught *P.*
1007 *papatasi* populations from PPAW, PPJM, and PPJS. (B) Weblogo illustrating the relative
1008 frequencies of amino acid polymorphisms in wild caught *P. papatasi* populations from PPAW,
1009 PPJM, and PPJS.
1010
1011 **S28 Table**. **PpSP42 population genetics analyses for *P. papatasi* populations**
1012 NS=$p>0.10$; NS[1]=$0.10 > p > 0.05$; *=$p<0.05$
1013
1014 **S29 Table. *PpSP42* pairwise comparisons of genetic differentiation estimates.**
1015
1016 **S30 Fig. Median-joining network for PpSP42 *P. papatasi* haplotypes.**

Circle size and circle color indicates frequency and geographical location of haplotypes, respectively. Haplotype numbers are written next to the corresponding circle H_XX. Red numbers between haplotypes indicate number of mutations between haplotypes.

S31 Table. PpSP42 sliding window analysis.

Ka/Ks were plotted for every 70 codons. Values greater than one suggest the potential for positive selection. ---- indicates a lack of polymorphic data in the window to calculate a Ka/Ks value.

S32 Fig. PpSp42 secondary structure, polymorphic sites, and MHC class II epitope predictions.

The mature PpSP42 amino acid sequence predicted secondary structure. Yellow highlighted amino acids indicate the predicted MHC class II predicted promiscuous peptides. Individual amino acids underlined in black indicate unique polymorphic sites. Predicted secondary structure based on sequence accession #AGE83094[13].

S33 Fig. PpSP44 nucleotide and amino acid variation.

(A) Weblogo illustrating the relative frequencies of nucleotide polymorphisms in wild caught *P. papatasi* populations from PPAW, PPJM, and PPJS. (B) Weblogo illustrating the relative frequencies of amino acid polymorphisms in wild caught *P. papatasi* populations from PPAW, PPJM, and PPJS.

S34 Table. **PpSP44 population genetics analyses for *P. papatasi* populations**

1040 NS=p>0.10; NS[1]=0.10 > p > 0.05; *=p<0.05

1041

1042 **S35 Table. *PpSP44* pairwise comparisons of genetic differentiation estimates.**

1043

1044 **S36 Fig. Median-joining network for PpSP44 *P. papatasi* haplotypes.**

1045 Circle size and circle color indicates frequency and geographical location of haplotypes,

1046 respectively. Haplotype numbers are written next to the corresponding circle H_XX. Red

1047 numbers between haplotypes indicate number of mutations between haplotypes.

1048

1049 **S37 Table. PpSP44 sliding window analysis.**

1050 Ka/Ks were plotted for every 70 codons. Values greater than one suggest the potential for

1051 positive selection. ---- indicates a lack of polymorphic data in the window to calculate a Ka/Ks

1052 value.

1053

1054 **S38 Fig. PpSp44 secondary structure, polymorphic sites, and MHC class II epitope**

1055 **predictions.**

1056 The mature PpSP44 amino acid sequence predicted secondary structure. Yellow highlighted

1057 amino acids indicate the predicted MHC class II predicted promiscuous peptides. Individual

1058 amino acids underlined in black indicate unique polymorphic sites. Predicted secondary structure

1059 based on sequence accession #AGE83095[13].

1060

1061 **S39 Table. Summary Tajima's D and Ka/Ks analysis for all *P. papatasi* salivary proteins**

1062 **studied.**

1063 NS=$p>0.10$; NS[1]=$0.10 > p > 0.05$; *=$p<0.05$

1064

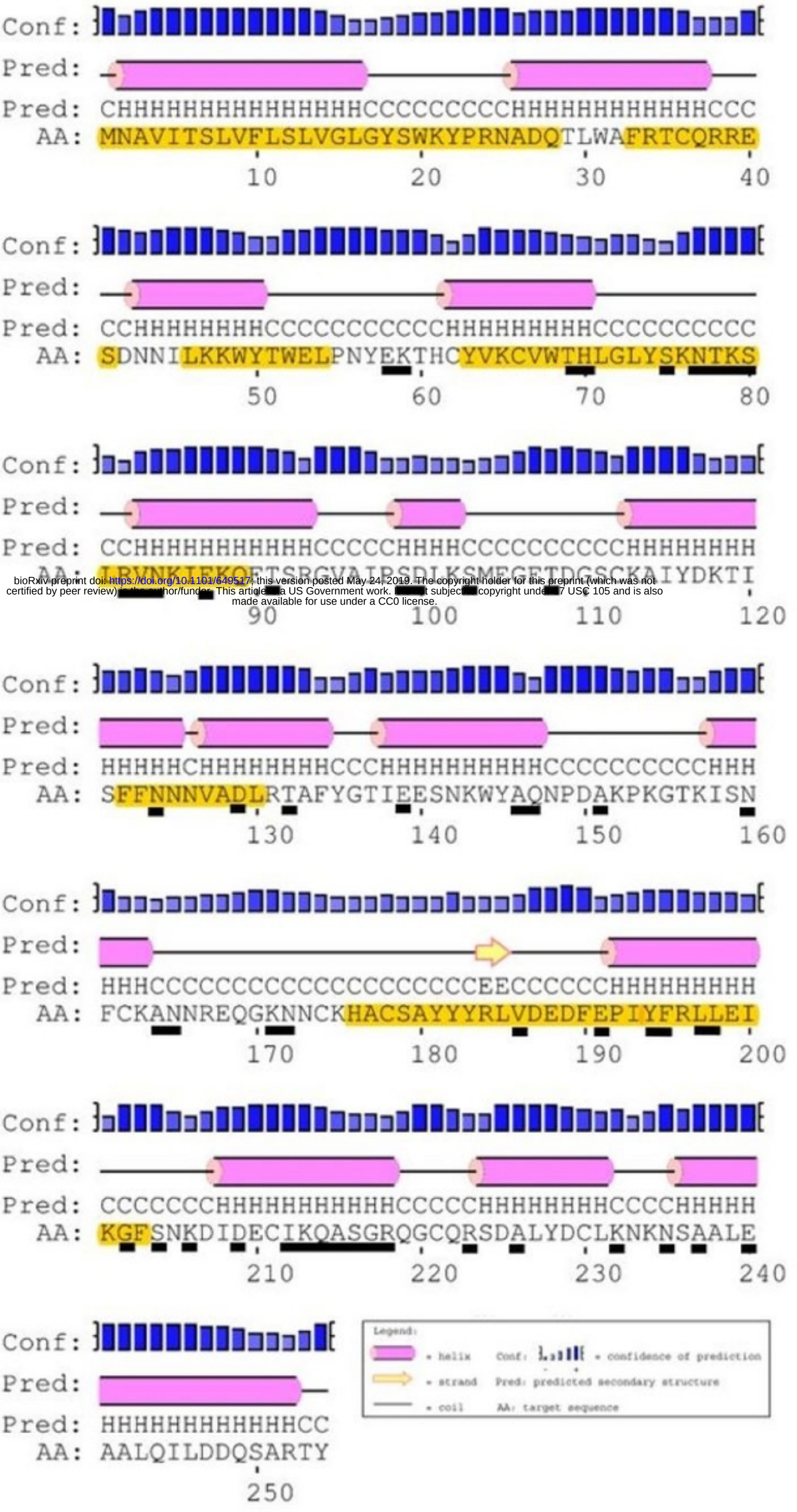

Figure 10

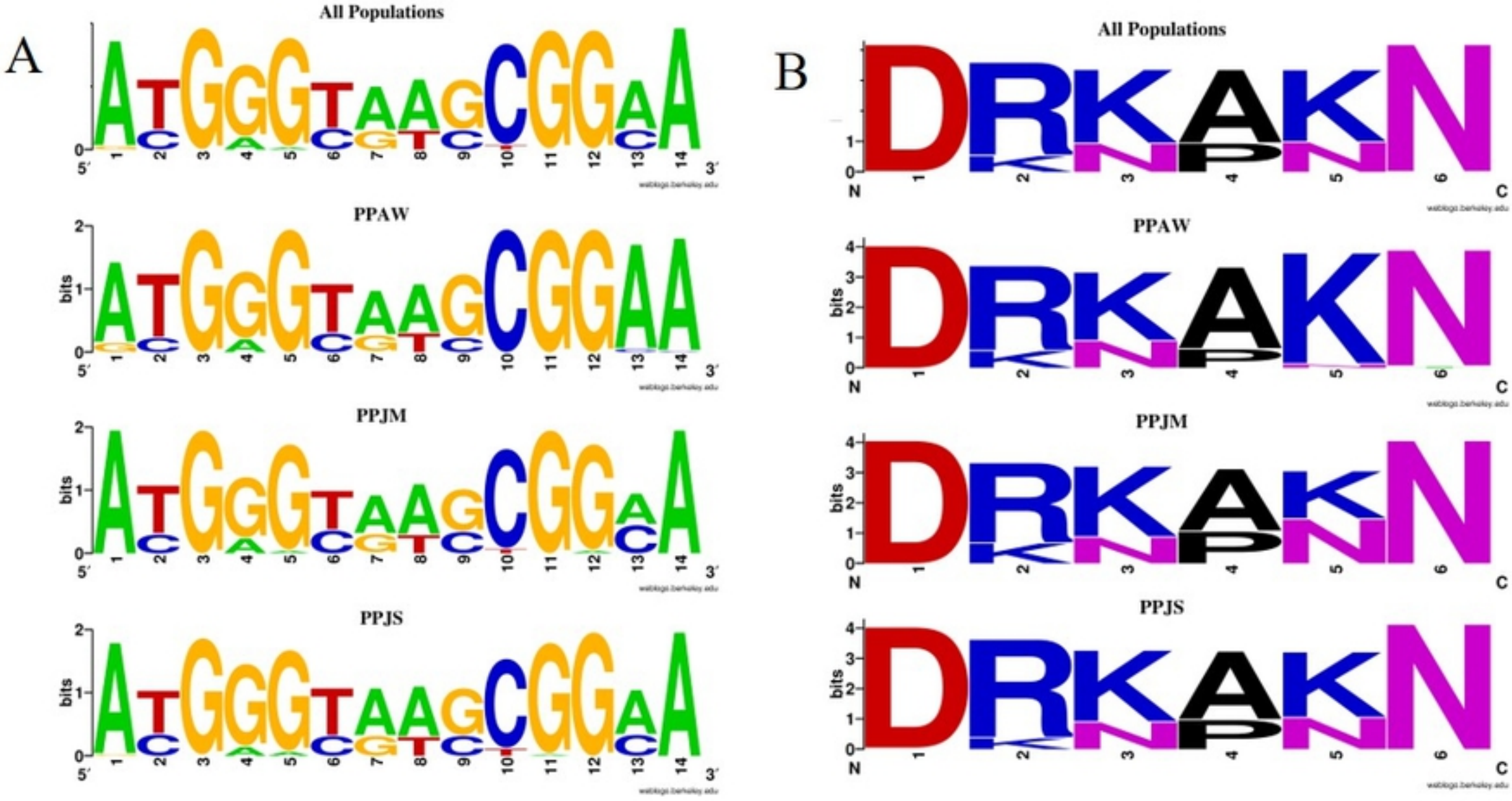
A
All Populations
PPAW
PPJM
PPJS
bits
5′
3′
B
All Populations
PPAW
PPJM
PPJS
bits
N
C

Figure 2

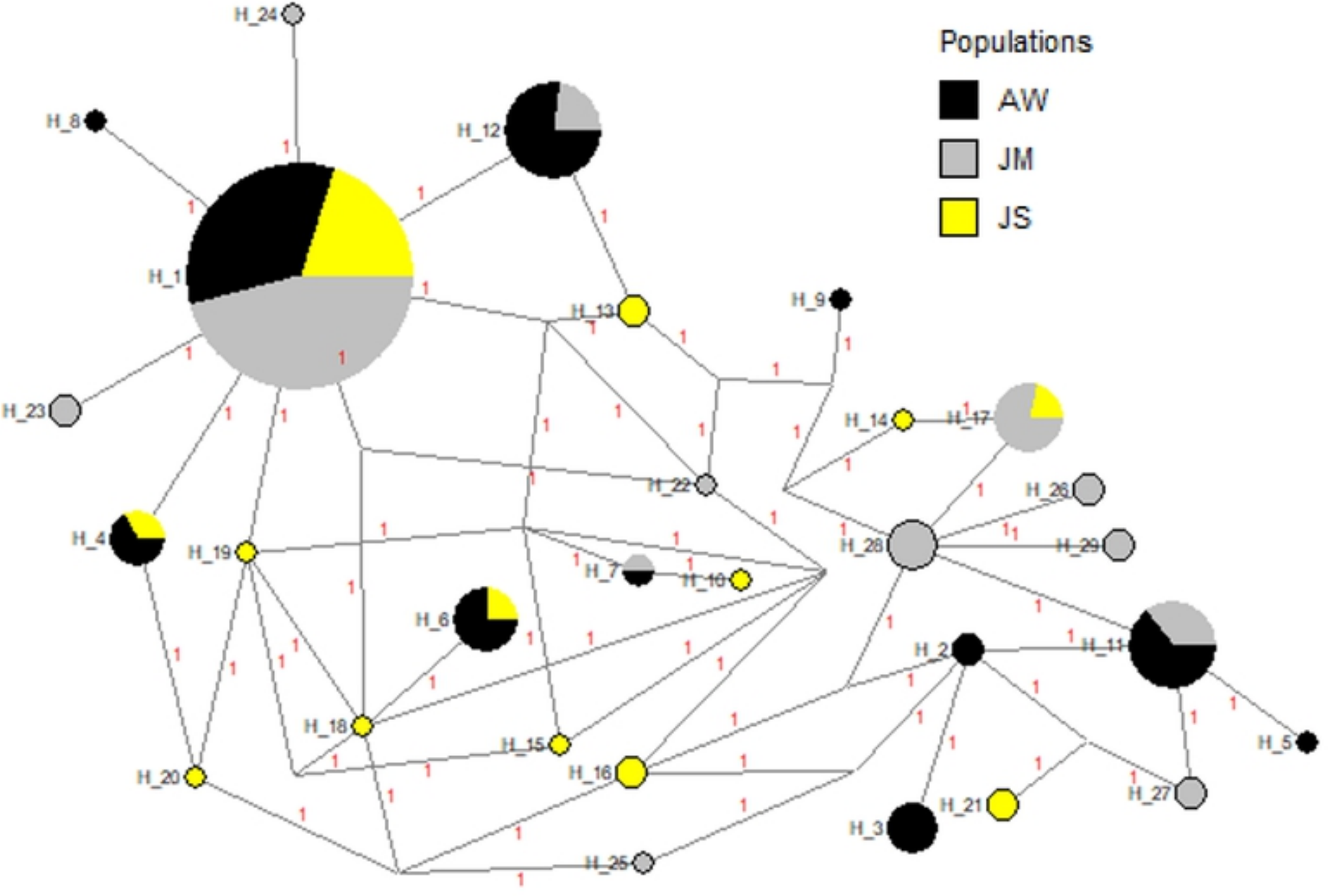
Populations
AW
JM
JS
H_24
H_8
H_12
H_1
H_13
H_9
H_23
H_14
H_17
H_22
H_26
H_4
H_19
H_28
H_29
H_7
H_10
H_6
H_11
H_2
H_18
H_15
H_5
H_20
H_16
H_27
H_21
H_3
H_25

Figure 3

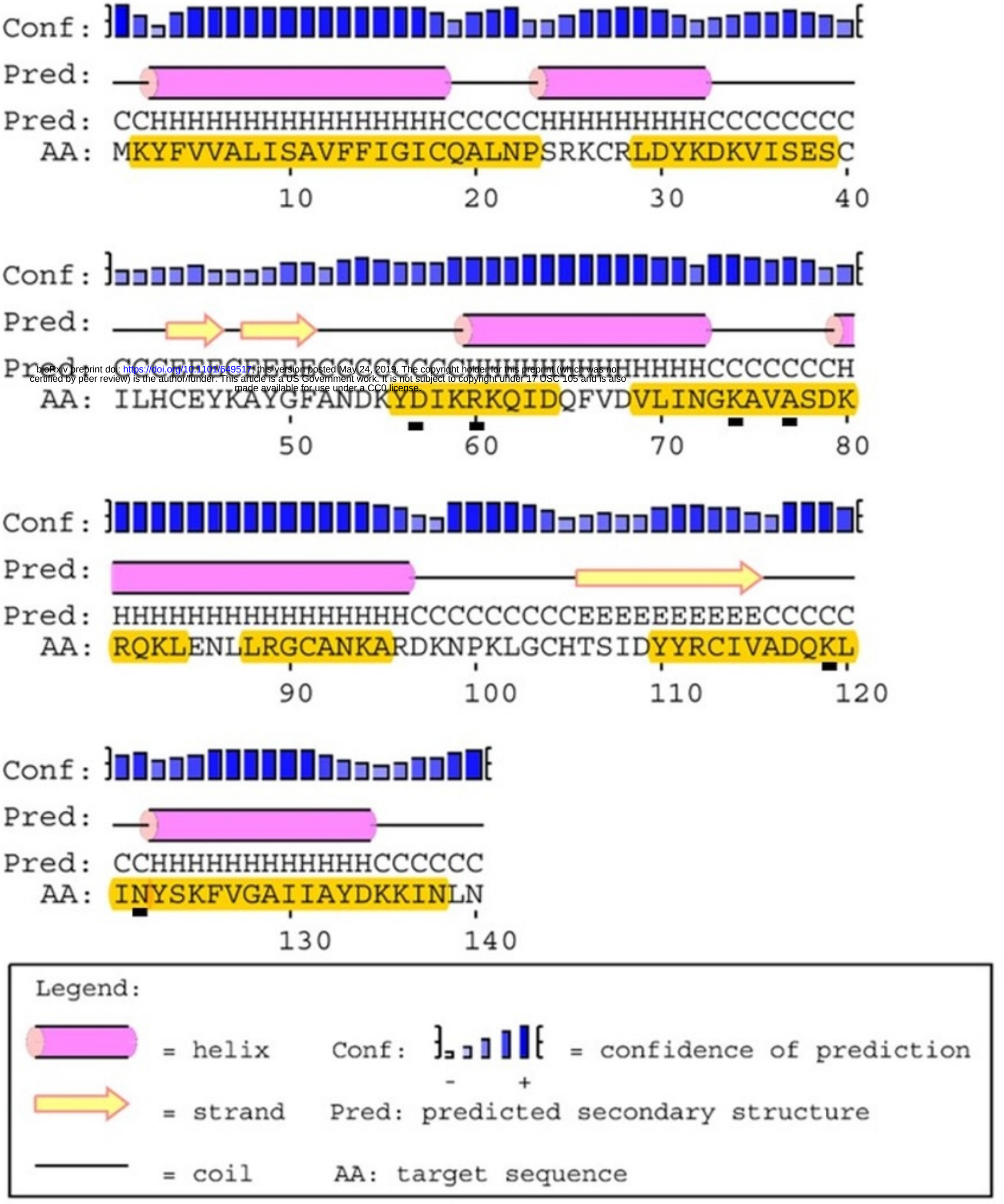

Figure 4

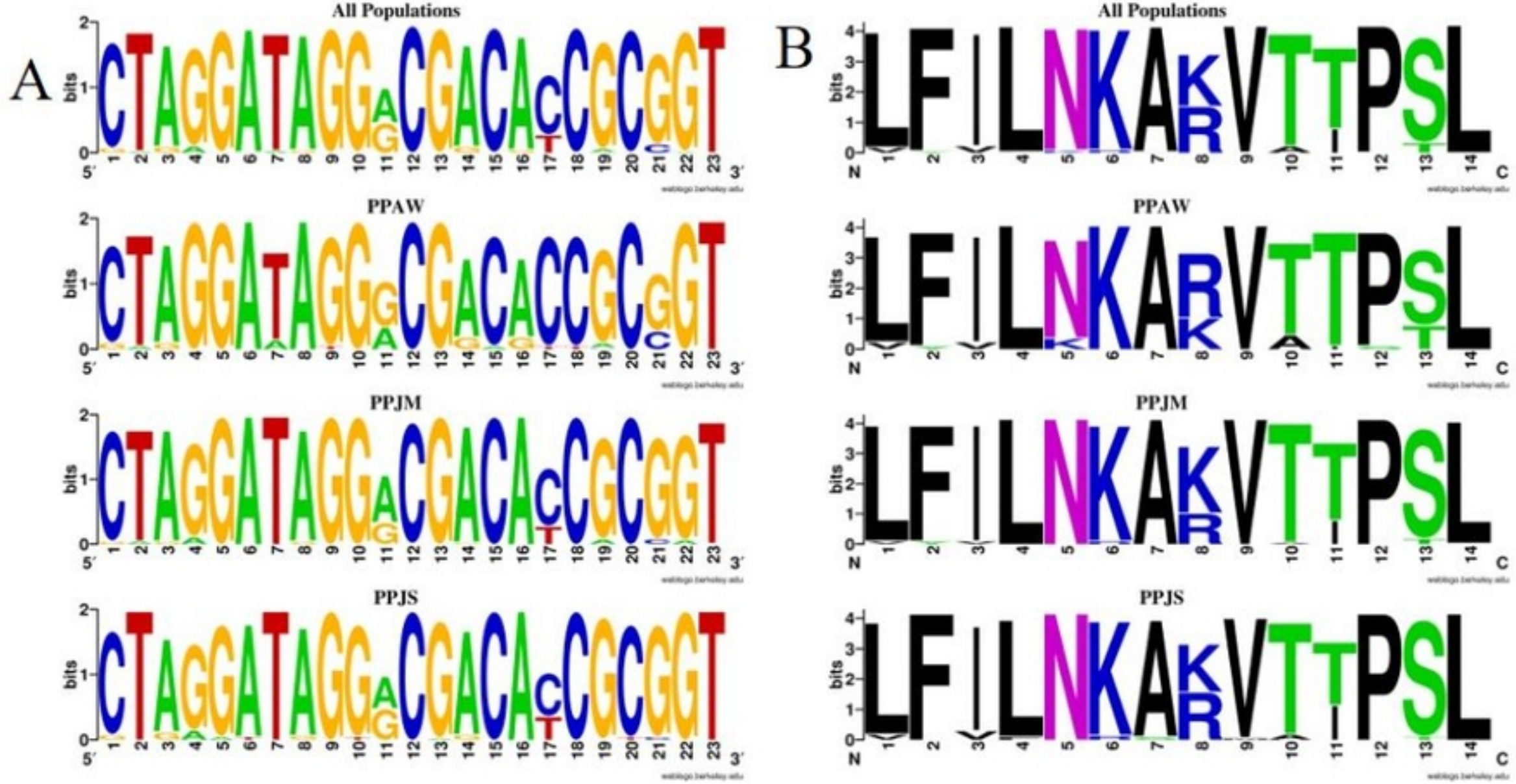
A
All Populations
PPAW
PPJM
PPJS
bits
5′
3′
B
All Populations
PPAW
PPJM
PPJS
bits
N
C

Figure 5

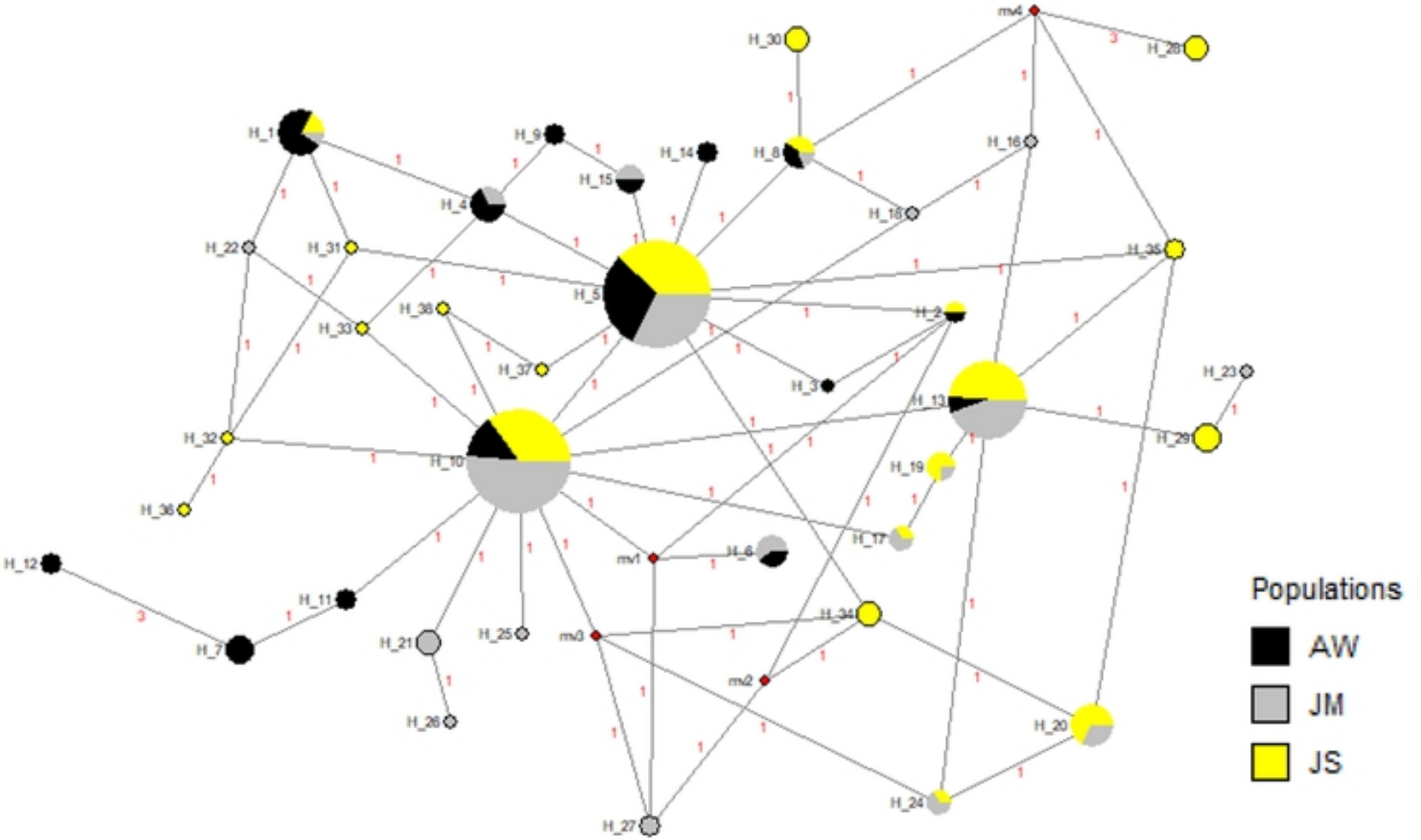
mv4
H_30
H_28
H_1
H_9
H_14
H_8
H_16
H_15
H_4
H_18
H_22
H_31
H_35
H_5
H_38
H_2
H_33
H_37
H_3
H_23
H_13
H_32
H_10
H_29
H_19
H_36
H_17
H_12
mv1
H_6
H_11
H_34
H_21
H_25
mv3
H_7
mv2
H_26
H_20
H_24
H_27
Populations
AW
JM
JS

Figure 6

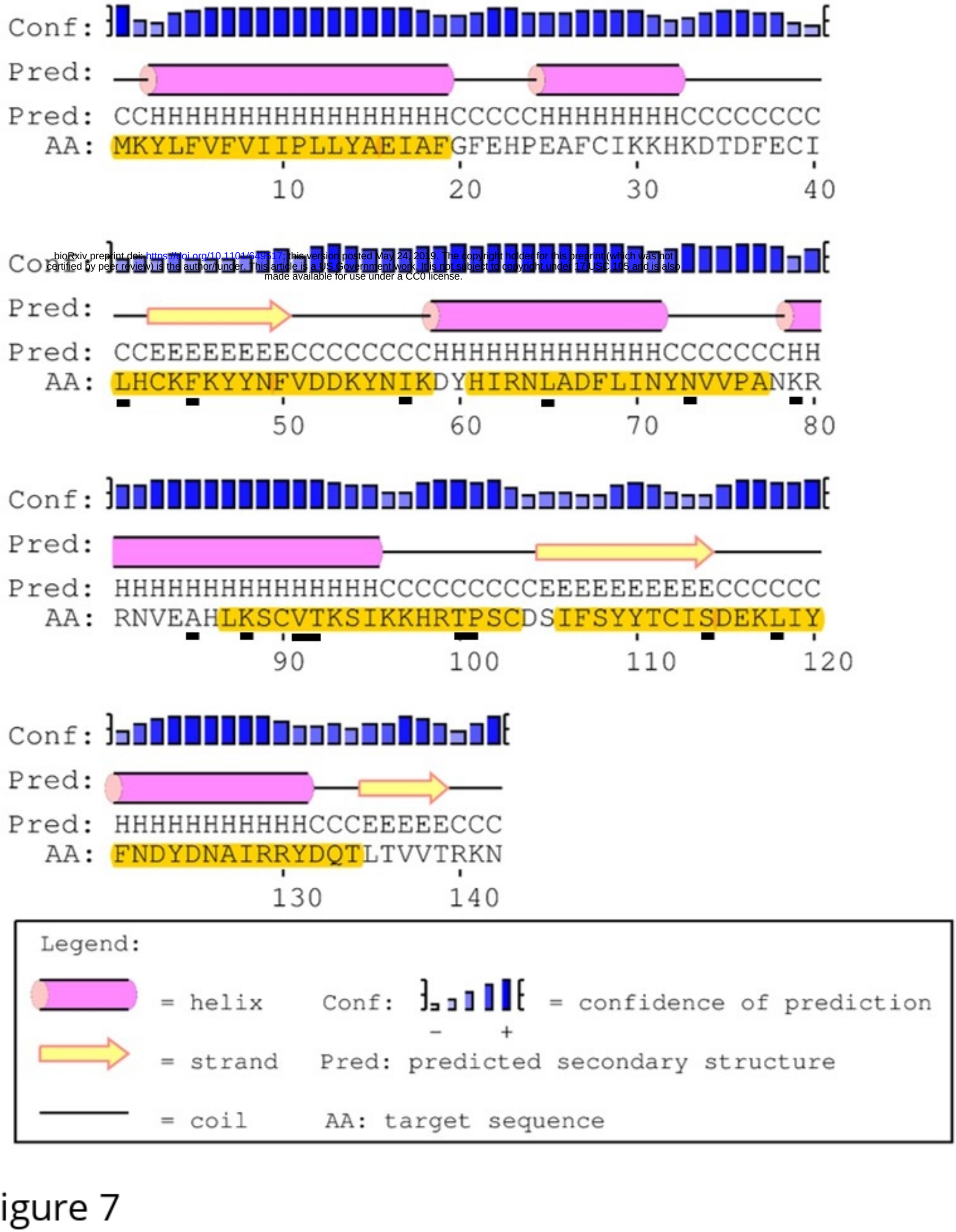

Figure 7

A

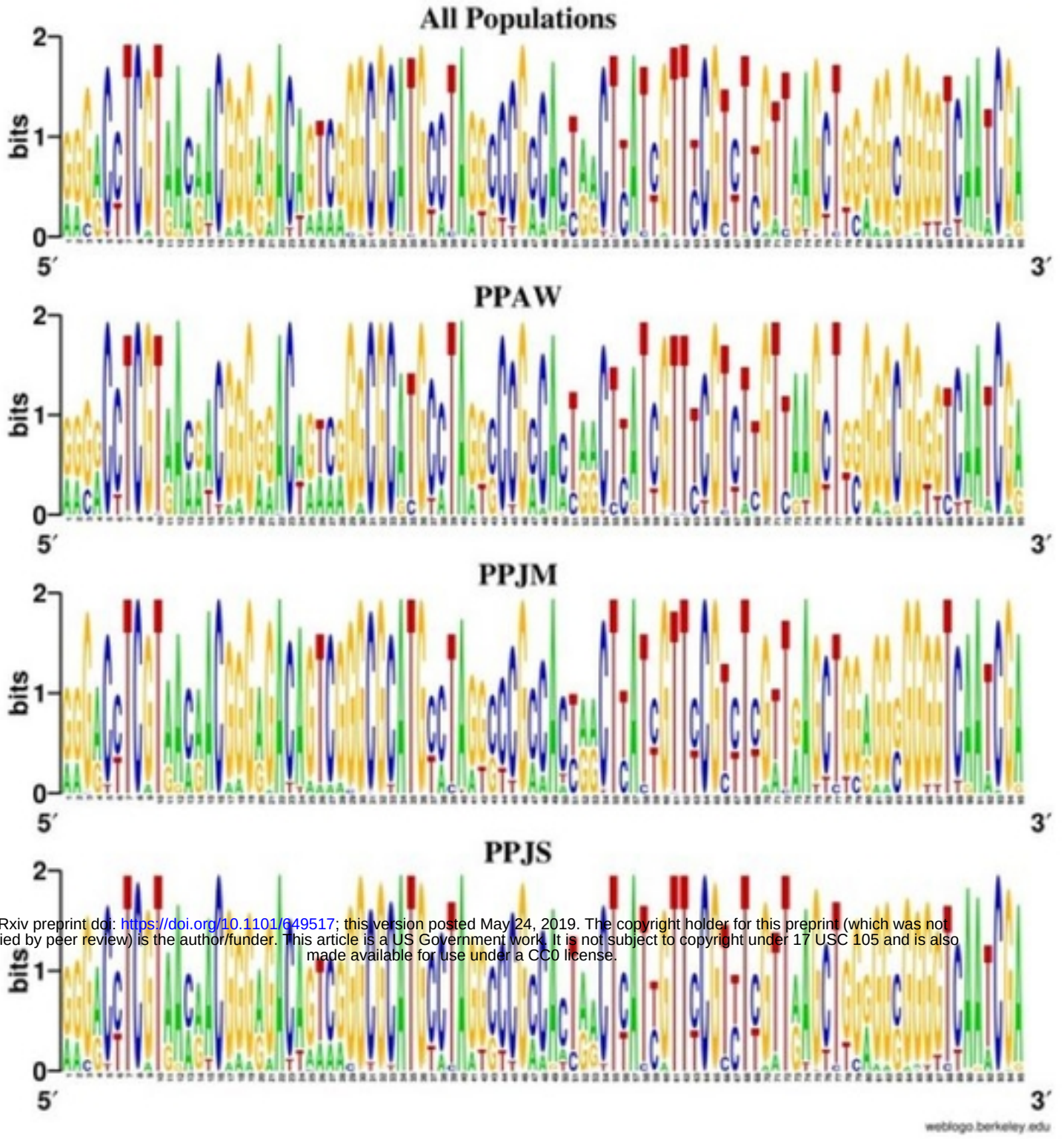

B

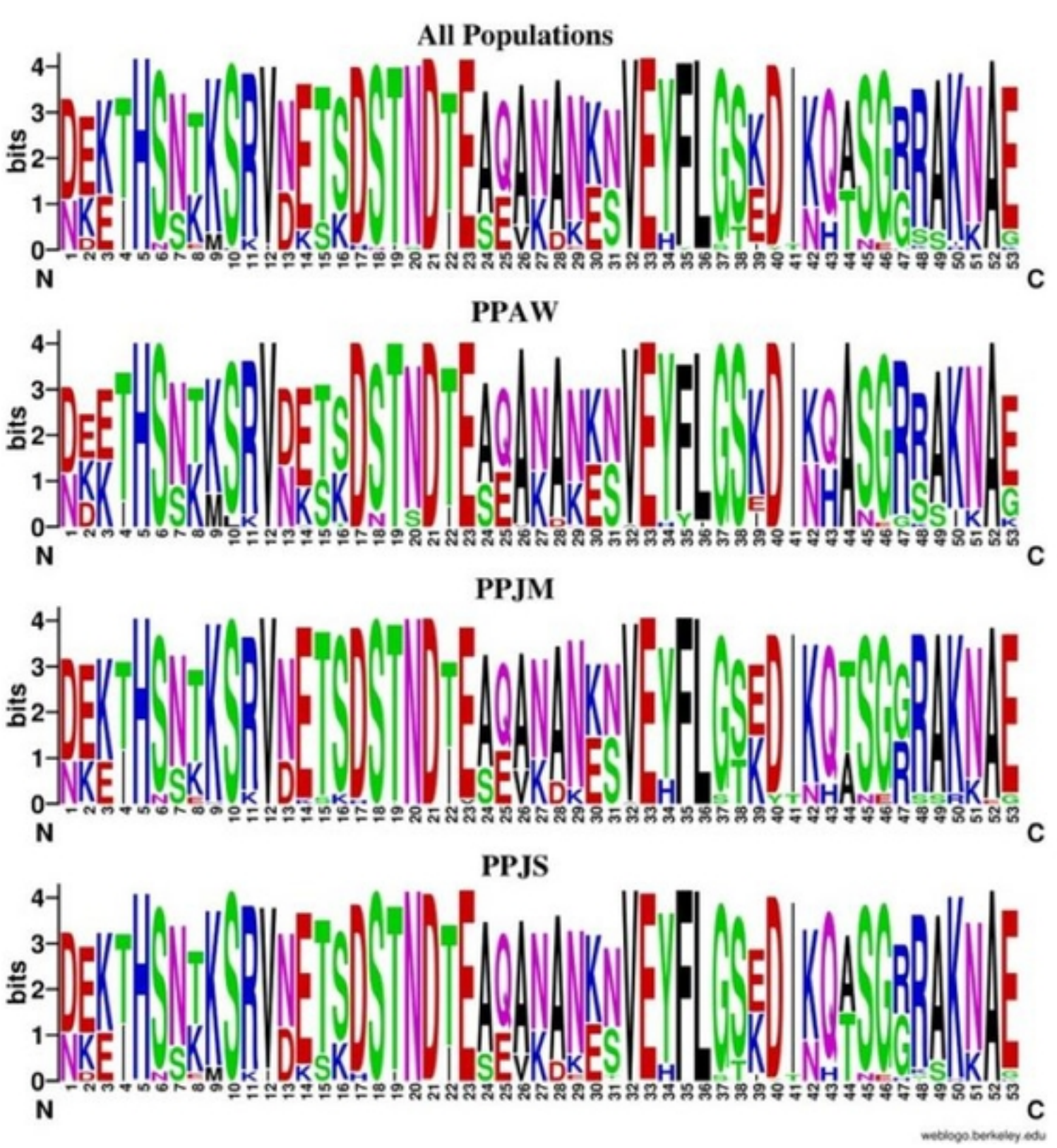

Figure 8

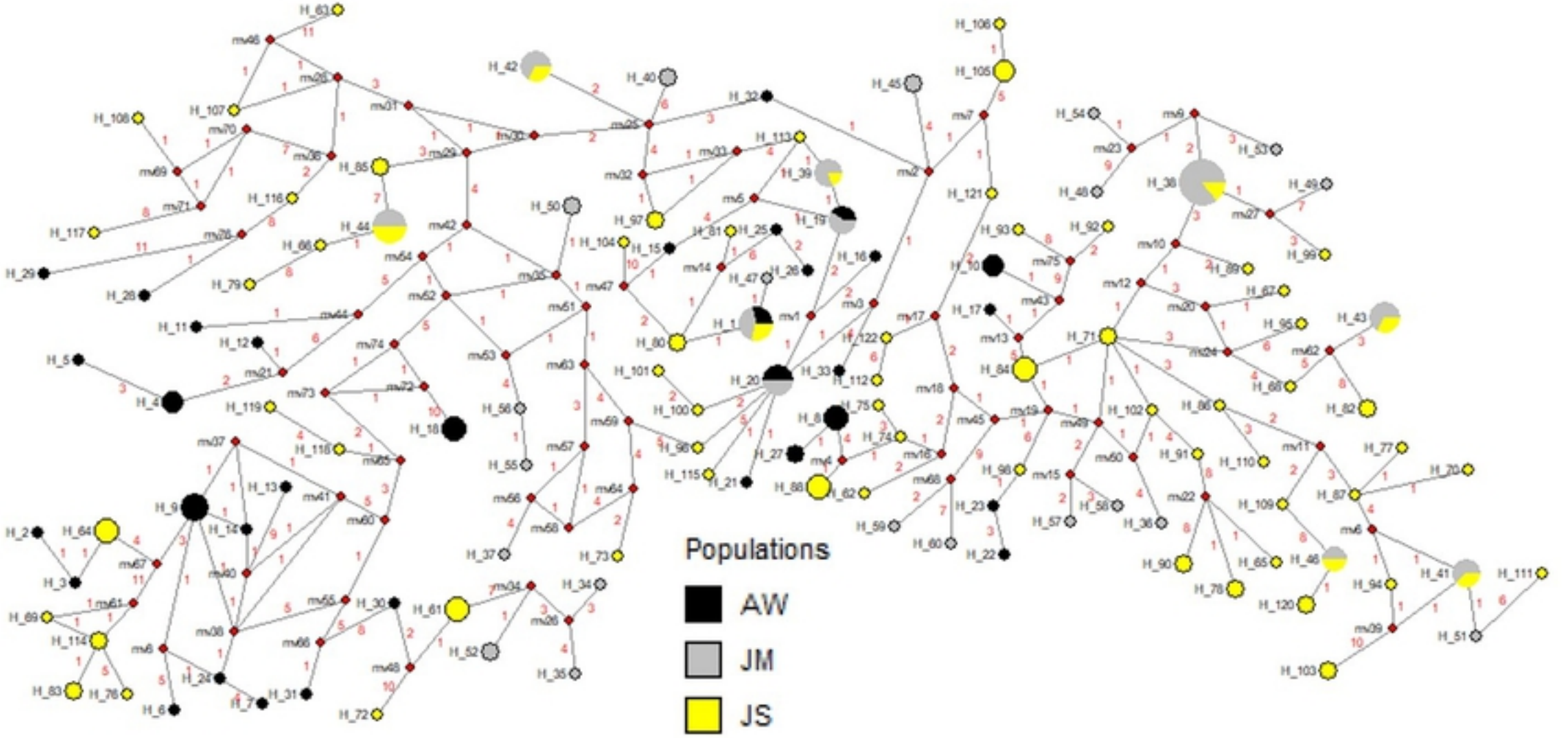

Figure 9

Figure 1